2016

Monitoring voltage stability margin across several transmission lines using synchrophasor measurements

Lina Marcela Ramirez Arbelaez
Iowa State University

Monitoring voltage stability margin across several transmission lines using synchrophasor measurements

by

Lina Marcela Ramirez Arbelaez

A dissertation submitted to the graduate faculty

in partial fulfillment of the requirements for the degree of

DOCTOR OF PHILOSOPHY

Major: Electrical Engineering

Program of Study Committee:

Ian Dobson, Major Professor

James McCalley

Manimaran Govindarasu

Umesh Vaidya

Venkataramana Ajjarapu

Iowa State University

Ames, Iowa

2016

TABLE OF CONTENTS

LIST OF TABLES

LIST OF FIGURES

ACKNOWLEDGEMENTS

I would like to use this opportunity to express my thanks to those who helped me with various aspects of conducting research and the writing of this thesis. First and foremost, Dr. Ian Dobson for his guidance, patience and support throughout this research and the writing of this thesis. His insights and words of encouragement have often inspired me and renewed my hopes for completing my graduate education.

I would be grateful to my committee members for their efforts and contributions to this work: Dr. Venkataramana Ajjarapu, Dr. James McCalley, Dr. Manimaran Govindarasu, and Dr. Umesh Vaidya.

I am absolutely grateful to my family, and Santiago for his love, support, and for having made my experience something more enjoyable during this years. Furthermore, I thank all the people from XM (Colombia ISO) that helped me, for all your support regarding the application of my thesis.

Additionally, I would like acknowledge for all the financial support from the Electric Power Research Center at Iowa State University, PSERC, Arend J. and Velma V. Sandbulte professorship funds, and NSF grant CPS-1135825.

ABSTRACT

Power systems are frequently exposed to large transfers of power between areas, which can increase the risk of voltage stability problems and blackout. In addition, multiple outages are more likely to occur during severe weather and cyber physical attacks, which can weaken the power system and also increase the risk of voltage stability problems and blackout. To address these problems, it is desirable to be able to quickly monitor voltage stability online for corridors vulnerable to voltage stability problems. It is useful to do this monitoring without running simulation or estimate the state because power systems are very complex and there is not enough time for running simulation for all the possible multiple outages, and the state estimator may not converge for some severe outages.

This thesis proposes two new methodologies for a fast online evaluation of voltage stability margin across several transmission lines and under multiple contingencies. The first methodology is based on the voltage across area reduction, and the second is based on the preservation of the complex power of the transmission corridor. Those methods are based on synchrophasor measurements, giving the operators a fast indication of voltage stability problems that is independent of state estimation. In addition, this thesis proposes a new voltage stability index that is tracking the maximum power that the corridor with multiple lines can transfer.

Current methods of voltage stability monitoring with syncrhophasor measurements work for a load supplied by a corridor with a radial single line. However, many practical situations involve load supplied by more complicated corridors with multiple transmission lines. Thus, this thesis shows how to reduce multiple corridors to a closely equivalent radial corridor, including the variation of all loads that are connected to the corridor. The monitoring method can easily accommodate changes in the generator reactive limits. Furthermore, we tested these methods with satisfactory results in several systems, including a real power system, and compared it with commercial software, obtaining excellent results.

CHAPTER 1. STATEMENT OF THE PROBLEM

1.1 Introduction

It is always necessary to operate the electrical power system to maintain stability and security. However, power grids are increasingly stressed, and it is more difficult to maintain the stability of power systems when they are being operated nearer to their stability limits. The reasons for this behavior are based in economic and environmental limitations, and the result is more problematic operation in real time of the bulk power transmission system.

One significant limitation, which is our interest, arises from the location of generation and load. Inexpensive, clean and abundant generation is generally distant from the load, creating the need that some areas export large quantities of power. The large transfer of power between areas increases the risk of voltage stability problems in which stability is lost, voltages fall, and blackout is caused. In addition, power systems are exposed to multiple outages due to severe weather and cyber physical attacks, which can make the power system vulnerable to voltage stability problems and blackouts. Other important problem arise in the planning process, it is not possible to account for all the possible outages due to the complexity of multiple outages and the economic cost of planning the system to account for them.

According to the issues mentioned, voltage instability problem is complex, and it is not easy to detect. If the voltage stability problem is not fixed rapidly and appropriately, it is difficult to restore stability, and the problem can turn into a voltage collapse and a blackout. In order to help solve those problem, this thesis describes two new methods and a new voltage stability index for monitoring in real time voltage stability margin using synchrophasor measurements, across transmission corridors with substantial transfers of power, and under multiple contingencies.

1.2 Motivation

Nowadays many corridors of a power system transport large amounts of power, which, although economically advantageous, stresses the system, changes the normal behavior, and in summary makes the system more susceptible to voltage stability problems. In addition, power system are complex, and they are exposed to multiple outages during bad weather condition or cyber attacks. Losing lines or elements of the grid make the power systems weak and with more risk of voltage collapse events and blackouts.

Voltage stability is a complex problem in real time because the magnitude of the voltage cannot be a good alarm during voltage stability difficulties. In fact, it is possible for voltage magnitudes to be maintained by reactive controls while the voltage stability problem is becoming more severe (8). In addition, when the system is close to or past the point of voltage collapse, it is very difficult to return the system to the stable point, even if more reactive power is injected (10). Voltage collapse can be detected and avoided by calculations based on the state estimator (28), (49), but there is scope for alternative and complementary monitoring, particularly since the state estimation and the calculations take some time to complete, and in some fault situations the state estimator is not reliable, and it is good to have another independent approach available.

All the reasons presented above are the motivation of this thesis. Developing an online application for fast monitoring of the voltage stability margin using syncrophasor measurements between areas with large transfers of power, and under multiple contingencies is the solution that we propose. The principal benefit will be a rapid warning, which will help the operator to respond promptly to voltage stability problems. This measurement based method will supplement and complement slower methods based on calculations dependent on the state estimator.

To explain better the problem and the solution of this thesis, Fig. 1.1 shows a power system with a corridor that connects the areas A and B to C. The corridor A-B to C is of interest because it transports a large amounts of power, areas A and B have large amounts of surplus generation, which is exported to area C.

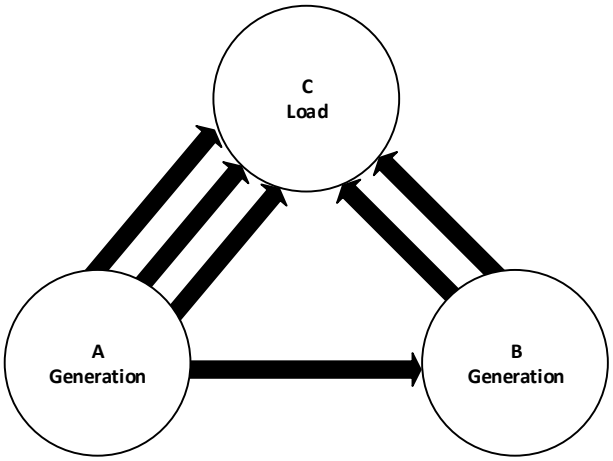

Figure 1.1 Corridor connecting three areas with several lines

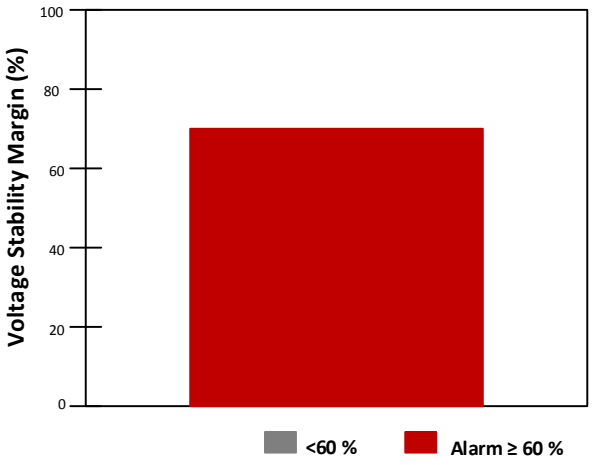

Figure 1.2 Proposed online voltage stability display for corridor AB-C

In Fig. 1.2 is shown a likely form of the application of this research. This example shows an alarm display that the operator would see in the control center video wall, which is indicating when the corridor AB-C is near to the instability point. In normal condition of the system, the display is gray but under a critical condition, the display turns red, alarming the operator.

1.3 The challenge

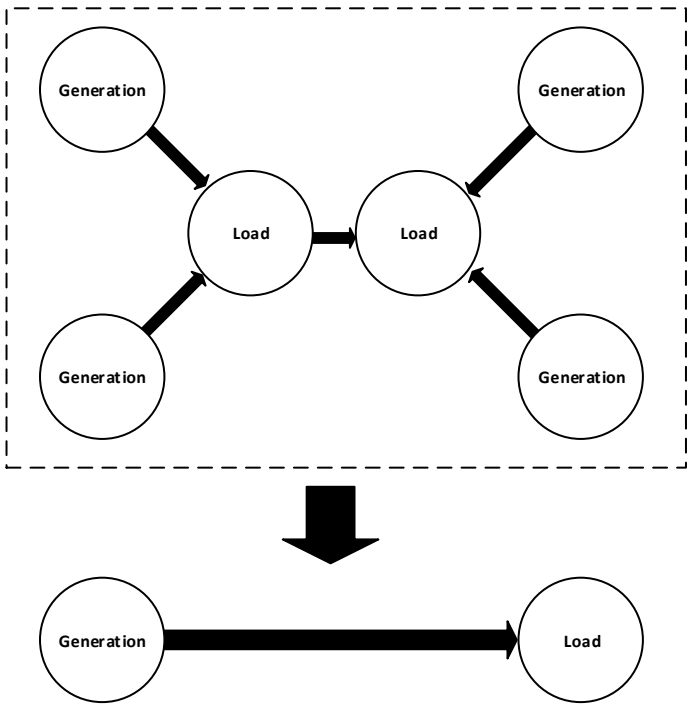

Figure 1.3 Combining multiple lines to a single line corridor

Currently it is possible to monitor voltage stability for a single line in real time (53),(24). However, in real world, power systems are usually not radial. In real systems there are several lines that connect areas, and several lines that enter load centers in order to satisfy their power requirements. Due to these problems, some researchers recognized the importance of developing an online voltage stability tool for a system with multiple transmission lines (55), (35), (39). However, those approaches require strong assumptions, such as known admittance between the loads or generators, capturing changes on the transmission corridor, or assuming known complex voltage in the generator. Those assumptions can generate inaccurate results, especially during multiple contingencies.

Thus, the challenge of this research is to find a well-founded approach to combine several lines, which connect two or more areas, into a single equivalent line to which the single line

method for voltage stability may be applied with confidence, see Fig. 1.3. All of this has the final goal of evaluating voltage stability using synchrophasor measurement units for a transmission corridor of a real systems, as is shown in Fig. 1.4.

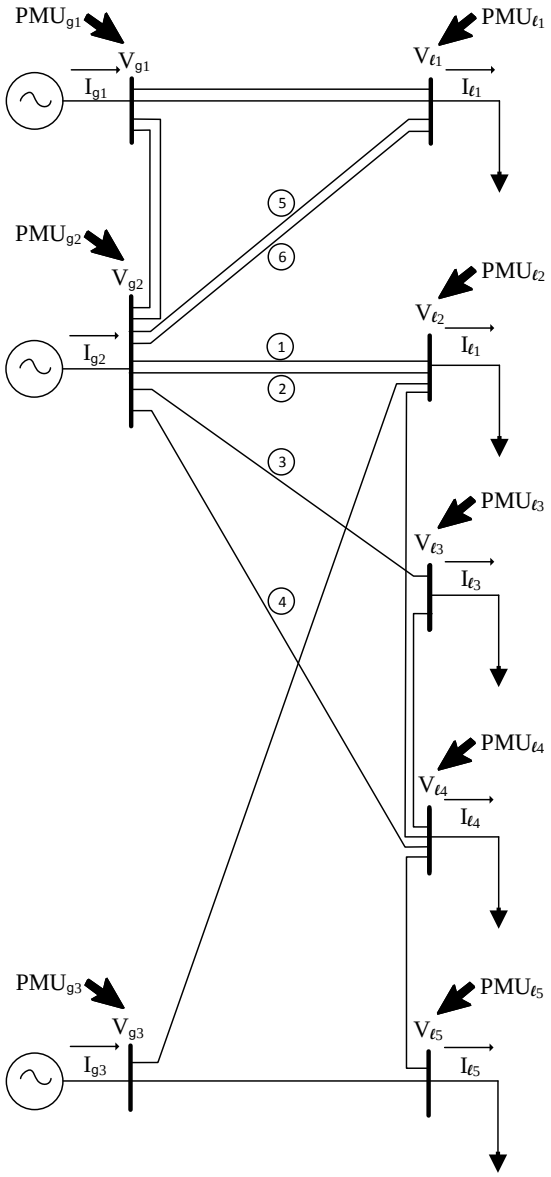

Figure 1.4 Transmission corridor of the Colombian Power System

1.4 Objectives

The general objective is designing a model for assessing real time voltage stability margin using synchrophasor measurements in corridors composed by several lines, with high transfers of power, and under multiple possible contingencies.

The specific objectives are:

1. Combine synchronized measurements and reduce a corridor with multiple lines to a single line.

2. Evaluate the voltage stability margin using synchrophasor measurements of a corridor with multiple lines.

3. Evaluate the bifurcation point of the complete system and its equivalent.

4. Include generator reactive limits in the synchrophasor measurements voltage stability method.

5. Analyze the synchrophasor measurements voltage stability method for multiple outages in the transmission corridor.

6. Analyze the synchrophasor measurements voltage stability method including load inside of the transmission corridor.

7. Set the secure voltage collapse margin for practical cases.

8. Test the synchrophasor measurements voltage stability method in a real system.

9. Compare the synchrophasor measurements voltage stability method with commercial software.

1.5 Thesis organization

This chapter has presented the motivating aspects of doing the work, the research problem and the objectives.

Chapter 2 is a literature review of the traditional and modern tools for assessing voltage stability, and some application for multiple contingencies.

Chapter 3 presents two methods for reducing multiple lines into a single line.

Chapter 4 presents a comparison between the well known REI equivalent and the equivalents proposed in Chapter 3.

Chapter 5 presents a new voltage stability index based on the maximum power that the transmission corridor can transfer without voltage stability problems.

Chapter 6 shows a methodology for evaluating voltage stability online for multiple corridors, and in addition includes a new approach for including generator reactive limits into the voltage stability tool.

Chapter 7 shows a methodology for evaluating voltage stability online for multiple corridors and multiple outages, where the method is compared against commercial software. In addition this chapter presents how to set the security voltage stability margin.

Chapter 8 presents the contributions and future work of this research.

CHAPTER 2. LITERATURE REVIEW

Since the 1980s, many researchers have been studying voltage stability problems. This chapter will summarize the basics of voltage stability assessment, the recent methodologies for doing voltage stability assessment using synchrophasor measurements, and methods for evaluating voltage stability under multiple contingencies.

2.1 Voltage stability problem

Voltage stability is the capacity of the system to preserve stable voltage under steady state, and during events. Also, voltage stability is related to the ability of the system to supply the load and maintain the equilibrium between the load and demand.

Voltage instability can take place in different times; the problem could be fast (seconds) or long (hours), (33):

- Transient time scale: It has fast variables, and it is caused by electromagnetic transients, motor stalling and power electronics. This type of voltage instability is in a time scale of seconds and requires the analysis of the fast dynamics of the system.

- Long time scale: It has slow variables, and can involve the load evolution, load tap changes, over excitation limiters, and automatically switched capacitors or reactors. This type of voltage instability has a time scale of more than ten second and often can be analyzed using the static equations of the system. This thesis address long time scale voltage stability collapse.

Voltage stability problems involve many variables (2), however some of the causes of this problem are

- Load increase.
- Generators, capacitor banks, or SVC reaching reactive power limits.
- Tap changes.
- Line outages.
- Generator outages.

2.2 Saddle node bifurcations

Voltage instability is a nonlinear problem (14), (27) and it can be analyzed locally using saddle-node bifurcation. As the parameters of the system change slowly, we get two equilibrium points for the voltage, and at the bifurcation point, those equilibria become one (27). Beyond the bifurcation point, there is not equilibrium and the dynamics makes the voltage collapse until there is a blackout.

The simplistic case to illustrate saddle node bifurcation is

$$\dot{x} = -x^2 + \lambda, \tag{2.1}$$

where the state variable is x and the parameter is λ. In this case, before the bifurcation, the system has two equilibrium points: stable node and saddle. With a changing in the parameter λ, the saddle and stable node approach each other, collide at the bifurcation, and disappear after the bifurcation. In Fig. 2.1, we can clearly see how as the parameter increase, the stable equilibrium and the saddle equilibrium moving closer until the bifurcation where they become one.

The theory of bifurcation says that under suitable generic conditions, saddle node bifurcation is essentially the same as the simple example of Fig. 2.1, but extends into multiple state space dimension and multiple parameters space dimension. The mathematical method that demonstrate this is Liapunov -Schmidt Reduction (26).

In this thesis, we use the static model for finding the bifurcation point of the system. References (14), (15) state that the static model implies bifurcation of the dynamic model.

Thus we can use only the static equations for finding the bifurcation point as well as the margin of voltage stability.

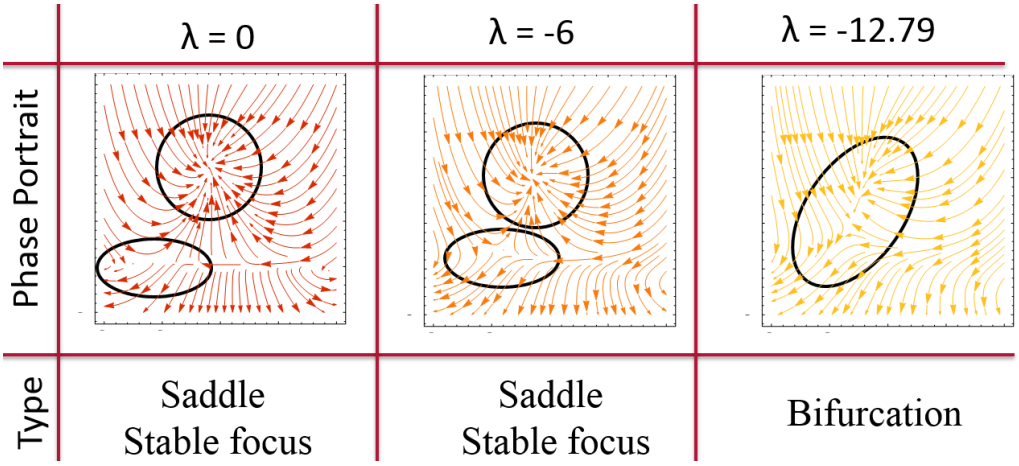

Figure 2.1 Saddle node bifurcation phase portrait

2.3 Tools for voltage stability analysis

In the literature we can find several methods for voltage stability analysis, such as P-V curve method, V-Q curve method and reactive power reserve method, methods based on singularity of power flow Jacobian matrix at the point of voltage collapse, direct method, and continuation power flow (1), (2), (8), (10).

In this thesis, we will use the continuation power flow for offline analysis, and testing.

2.3.1 Continuation power flow

The continuation power flow is a methodology for finding the bifurcation point using power flow, the predictor and corrector, (1). The steps for doing that are

1. Run conventional power flow on the base case.
2. Specify the continuation parameter, the state variable with the largest tangent vector component.
3. Calculate the tangent vector, for this case λ is the continuation parameter, and λ is assumed increasing.

$$\begin{pmatrix} F_\delta & F_v & F_\lambda \\ & & \\ 0 & 0 & 1 \end{pmatrix} \begin{pmatrix} d\delta^{(0)} \\ dV^{(0)} \\ d\lambda^{(0)} \end{pmatrix} = \begin{pmatrix} 0 \\ 0 \\ \pm 1 \end{pmatrix} \tag{2.2}$$

4. Predict the solution, where σ is a specified step length.

$$\begin{pmatrix} \delta^{(1)} \\ V^{(1)} \\ \lambda^{(1)} \end{pmatrix} = \begin{pmatrix} \delta^{(0)} \\ V^{(0)} \\ \lambda^{(0)} \end{pmatrix} + \sigma \begin{pmatrix} d\delta^{(0)} \\ dV^{(0)} \\ d\lambda^{(0)} \end{pmatrix} \tag{2.3}$$

5. Correct the prediction, for this step we should substitute the values obtained in the prediction into the power flow equations, and we obtain the mismatch ΔF. Then the corrector is

$$\begin{pmatrix} \Delta\delta^{(1)} \\ \Delta V^{(1)} \\ \Delta\lambda^{(1)} \end{pmatrix} = - \begin{pmatrix} F_\delta & F_v & F_\lambda \\ & & \\ 0 & 0 & 1 \end{pmatrix}^{-1} \begin{pmatrix} \Delta\delta^{(1)} \\ \Delta V^{(1)} \\ \Delta\lambda^{(1)} \end{pmatrix} \tag{2.4}$$

6. Using the predictor and corrector, the corrected solution is

$$\begin{pmatrix} \delta^{(1)} \\ V^{(1)} \\ \lambda^{(1)} \end{pmatrix} = \begin{pmatrix} \delta^{(1)} \\ V^{(1)} \\ \lambda^{(1)} \end{pmatrix} + \sigma \begin{pmatrix} \Delta\delta^{(1)} \\ \Delta V^{(1)} \\ \Delta\lambda^{(1)} \end{pmatrix} \tag{2.5}$$

7. Repeat the procedure until the bifurcation point is detected by (2.5).

2.4 Reduction for voltage instability analysis

For offline studies is desired to reduce multiple bus systems to a small system in order to reduce computation time. Many methods have been proposed for combine several PV buses

to a single bus (57), where the REI equivalent (13), and dynamic transient equivalent (44) are well known. One reduction differs from the methods mentioned before, proposing a method for reducing big systems which is very useful for voltage stability analysis because it is not depending on the base case voltages and power flow (37).

2.5 Benefits of real time monitoring

Applications using synchrophasor measurements are improving the way of managing and operating the power systems. These kind of applications are making possible monitoring the dynamics of the power system online, with real data and without the problems and delays of running simulations. Some of the general benefits of those applications are

- Post-Disturbance Analysis (42).
- Power system restoration (42).
- Real time monitoring and control (42).
- Reliable protection schemes (58).
- Tracking the voltage angle (7), (12).
- Validation of power system models (31).

In summary, real time monitoring using synchrophasors is making possible early detection of power system problems, including the voltage stability applications that are considered as a critical need of the industry in order to prevent severe problems in the grid (24), (43).

2.6 Synchrophasor measurements to detect voltage stability problems in real time for radial cases

There is extensive previous work about monitoring the voltage collapse margin in real time on a single line with synchrophasor measurements near the load; see (53),(24), and references therein. These single line methods can apply nicely in the simpler radial situations.

Assuming that the load is constant power, the voltage collapse occurs as a condition of maximum power transfer to the load at which the load impedance and the Thévenin impedance of the line viewed from the load are equal in magnitude. The load impedance can be estimated directly from the synchrophasor measurements, and multiple synchrophasor measurements at closely spaced times are made to estimate the Thévenin impedance, using iterative methods (least squares (53), recursive least square (38), least square including filter for transients (23), least square and transformer tap position changes (18), triangulation (48), recursive least square (4; 38), Tellegen's theorem (47)), non-iterative methods (5), and replacing some of the PMU measurements with Thévenin impedance calculated from line status information from the state estimator (19).

The timing of the successive measurements needs to be small enough that the Thévenin impedance remains sufficiently constant, and needs to be large enough that changes in the load make the successive measurements change enough. Fulfilling these conditions can sometimes pose problems or require sophisticated corrections, especially during transient changes in the Thévenin equivalent caused by generation and transmission events (22). To avoid these problems, we will follow (35) in making simultaneous measurements at both the generation and load ends of the transmission line. Fig. 2.2 shows the single line case.

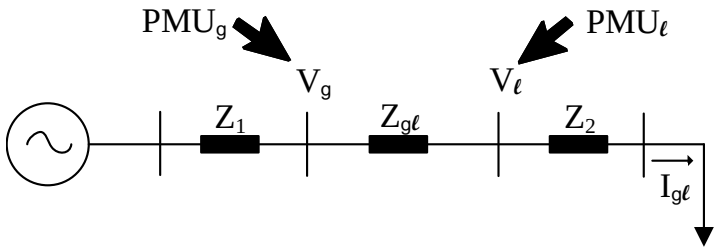

Figure 2.2 Single line system

First, it is important to clarify that this approach models the generator as PV, and as assumed in all the previous methods, the load is modeled as PQ. For this reason the state vector of the system is $x = \{\delta_g, V_\ell, \delta_\ell\}$, and the parameters are $\lambda = \{P_\ell, Q_\ell\}$. The parameter λ is supposed to vary more slowly than the dynamics, and the dynamics of the parameters are

neglected. The constant power assumption of PQ loads makes the voltage index conservative, underestimating the margin.

We combine the synchrophasor complex voltages and currents to estimate the Thévenin impedance according to

$$Z_{g\ell} = \frac{V_g - V_\ell}{I_{g\ell}}, \tag{2.6}$$

$$Z_\ell = \frac{V_\ell}{I_{g\ell}}. \tag{2.7}$$

Our intention is to apply this methodology to large transmission corridors with long lines of substantial impedance, where the corridor is defined as a set of transmission lines between the generators and load. Then the impedance Z_1 between the corridor and generation, and the impedance Z_2 between the corridor and the loads are relatively small, so that the equivalent impedance of the transmission corridor is approximately equal to the Thévenin impedance.

2.7 Voltage stability assessment for transmission corridors

Currently many researchers are trying to find the voltage stability margin for corridors formed from several transmission lines. The approaches that can be found in the literature are

- Voltage stability in a single load including the influence of the near loads, assuming known the admittance between the loads or generators (55). The issue with this approach is the assumption of the admittance between loads and generation. The reason is that when the lines between generation or load trip, have compensation, or under voltage tap changes, the impedance of the line changes, but the model is not capturing the modification. Those changes can make a substantial error in the index giving an incorrect voltage margin.

- Thévenin equivalent without iteration, using measurements at both the generation and load ends of the transmission line (35). The issue with this methodology is that the voltages are an average of the boundary voltages, making the model imprecise.

- Reduction of the system using Thévenin equivalents outside of the transmission corridor, where the admittances of the transmission corridor are known. The voltage stability

assessment could be done two ways: Making a Thévenin equivalent of each load, or analyzing the voltage stability of each load and when one of them is not stable the system is not stable (39). This method is a voltage stability evaluation of load by load, and has the problem of making constant all the loads, except the load that is analyzed, which is not realistic.

2.8 Voltage stability index

There are many stability indexes in the literature, and some of the most relevant are

- Index tracking the absolute value of the load impedance (41), (53), (36).
- Index using maximum transfer of power. Namely, equating the voltage of the load bus and the voltage drop in the Thévenin impedance (38).
- Index based on power, and assuming that loads are a function of time (4), (18).
- Index using the steady state and transient load power (6).
- Index based on reactive power (11).
- Index based on maximum transfer of power (25).
- Index based on maximum power using the cubic spline extrapolation technique (32).
- Index tracking the change of reactive power with the increment of the transfer of power (51).

The most used index is based on the fact that the maximum transfer of power occurs when the voltage of the load bus is equal to the voltage drop in the Thévenin impedance (38):

$$\text{Index} = \frac{\mid V_{g\ell} \mid 100}{\mid V_{\ell} \mid}. \tag{2.8}$$

Index (2.8) indicates the distance of the system to the bifurcation point, where 100% means voltage instability.

2.9 Contingency analysis

This subsection reviews some of the extensive previous work on off-line n-1 contingency screening for voltage collapse, see (20), (21), (29), (30), (40), and references therein.

During the 80s, the first procedures for finding the buses with potential voltage stability problems under contingencies, is based on power flow and modifications in reactive power consumption of the remaining system (20). Later, an efficient methodology for evaluating the change of the voltage collapse margin under contingencies is developed, which is based on the current operating point and the load forecast (29). The bifurcation and the load margin are computed and the load margin sensitivity to line outages is evaluated.

In (21), the sensitivity method is improved using a continuation power flow. A new index is proposed that includes the maximum load flow of the remaining lines and the sensitivities of the load margin under line outages. The method is further improved in (56), by using a two parameter continuation power flow, where one parameter is the load increase pattern and the other parameter controls the line outage.

The approach that we will present in this thesis differs from the methodologies previously mentioned, in using post-contingency measurements online rather than pre-contingency calculations based on the state estimator. Our synchrophasor measurement based approach can work independently of the state estimator. It is fast, and handles multiple contingencies more easily.

CHAPTER 3. REDUCTION OF A TRANSMISSION CORRIDOR WITH MULTIPLE LINES TO A SINGLE LINE EQUIVALEN

3.1 Method 1: Voltage across an area reduction

3.1.1 Introduction

In this section, we apply the new concept of the voltage across an area that is described in (17). The area voltage is a single complex number describing the voltage between the generators and loads that is consistent with circuit laws. In particular, in this section, the equivalent voltage across a single line is obtained by regarding the multiple transmission lines as an area of the power system, through which the generators supply the loads, and then combining the voltage measurements to obtain the voltage across the area.

3.1.2 Reduction

The equivalent is analyzed in a four bus system with two inputs (generators at bus $g1$ and $g2$) and two outputs (loads at bus $\ell 1$ and $\ell 2$), see Fig. 3.1, that will be reduced to an equivalent system with one input and one output, see Fig. 3.2. The equivalent assumes that all the power is going from the generation to the load. Equivalently, it assumes equal voltages at the generation and equal voltages at the load.

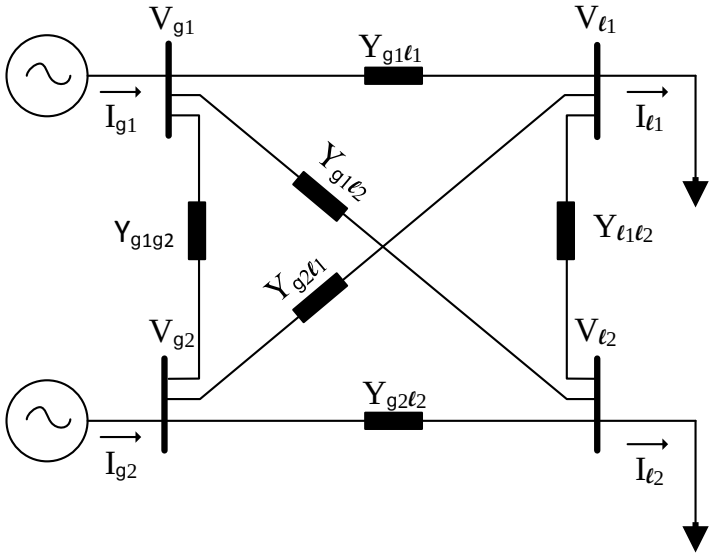

Figure 3.1 Power system with 2 inputs and 2 outputs and 6 lines corridor.

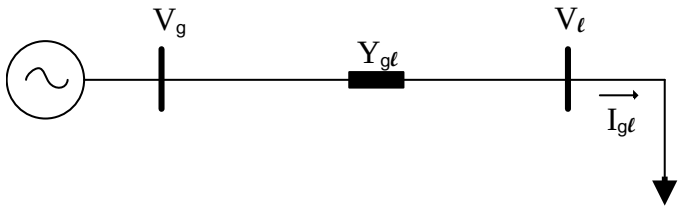

Figure 3.2 Reduced power system.

The equivalent is based on the combination of the voltages, according to the weights of the transmission lines that are connected in each bus. In this case, the reduction accounts for the admittance $Y_{gi\ell i}$, and neglects the admittances Y_{gigi} and $Y_{\ell i\ell i}$, with $i = 1, 2$. Accordingly, the weights for combining the admittance are:

$$w_{g1} = \frac{Y_{g1\ell1} + Y_{g1\ell2}}{Y_{g\ell}}, \tag{3.1}$$

$$w_{g2} = \frac{Y_{g2\ell1} + Y_{g2\ell2}}{Y_{g\ell}}, \tag{3.2}$$

$$w_{\ell1} = \frac{Y_{g1\ell1} + Y_{g2\ell1}}{Y_{g\ell}}, \tag{3.3}$$

$$w_{\ell2} = \frac{Y_{g1\ell2} + Y_{g2\ell2}}{Y_{g\ell}}. \tag{3.4}$$

Where

$$Y_{g\ell} = Y_{g1\ell1} + Y_{g1\ell2} + Y_{g2\ell1} + Y_{g2\ell2}. \tag{3.5}$$

Combine the complex current into the equivalent line current:

$$I_{g\ell} = I_{g1} + I_{g2}. \tag{3.6}$$

Combine measurements of complex voltage into the equivalent voltage at both ends of the single line:

$$V_g = w_{g1}V_{g1} + w_{g2}V_{g2}, \tag{3.7}$$

$$V_\ell = w_{\ell1}V_{\ell1} + w_{\ell2}V_{\ell2}. \tag{3.8}$$

3.1.3 Assumption and modeling

As was mentioned before, voltage collapse monitoring with synchrophasors for a single line is very convenient for radial systems. However, in the real world, the power system is usually not radial. In real systems, there are several transmission lines that connect generators to load centers in a somewhat meshed fashion in order to satisfy their power and reliability requirements. Thus, one of the challenges of this thesis is to combine several transmission lines into an equivalent single line where the single line method for voltage stability can be applied with confidence. In this chapter, we analyze a system with two inputs (generators at bus $g1$ and $g2$) and two outputs (loads at bus $\ell1$ and $\ell2$), see Fig. 3.3, that will be reduced to a system with one input and one output.

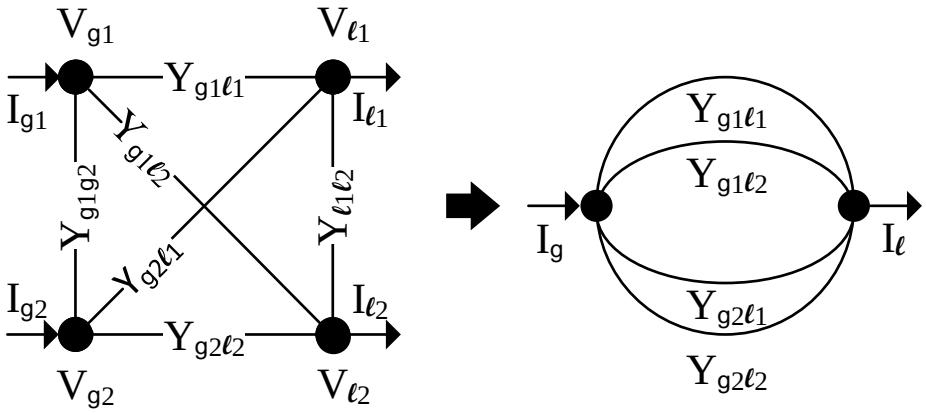

Figure 3.3 Reduction of power system with 2 inputs and 2 outputs.

Power networks have many degrees of freedom in their voltages and currents. Here we focus on one degree of freedom in which the generator voltages are equal, the load voltages are equal, and the total current into the transmission corridor is preserved. This transmission corridor degree of freedom describes the overall transfer of power from the generation to the load through the transmission corridor. For this degree of freedom of the network, we suppose that equal generator voltage at bus $g1$ and $g2$ is V_g, equal load voltage at bus $\ell 1$ and $\ell 2$ is V_ℓ, and the total current into the transmission corridor is $I_g\ell$.

On the corridor degree of freedom, equal voltages at bus $g1$ and $g2$ imply that bus $g1$ and $g2$ can be contracted or merged into a single bus g. Similarly, equal voltages at bus $\ell 1$ and $\ell 2$ imply that bus $\ell 1$ and $\ell 2$ can be contracted into a single bus ℓ. Since the transmission lines in the corridor are now in parallel between bus g and bus ℓ, the admittance between bus g and bus ℓ is given by (3.5), and it follows, see Fig. 3.3, that:

$$I_g = Y_{g\ell}(V_g - V_\ell). \tag{3.9}$$

Now the total current entering the transmission corridor is

$$I_{g1} + I_{g2} = (V_{g1} - V_{\ell 1})Y_{g1\ell 1} + (V_{g1} - V_{\ell 2})Y_{g1\ell 2} + (V_{g2} - V_{\ell 1})Y_{g2\ell 1} + (V_{g2} - V_{\ell 2})Y_{g2\ell 2}. \tag{3.10}$$

We want the current (3.9) entering the corridor in the corridor degree of freedom to be equal to the total current (3.10) entering the corridor in the entire network:

$$I_g = I_{g1} + I_{g2}, \tag{3.11}$$

which can also be expressed as

$$Y_{g\ell}(V_g - V_\ell) = (V_{g1} - V_{\ell 1})Y_{g1\ell 1} + (V_{g1} - V_{\ell 2})Y_{g1\ell 2} + (V_{g2} - V_{\ell 1})Y_{g2\ell 1} + (V_{g2} - V_{\ell 2})Y_{g2\ell 2}. \tag{3.12}$$

Now we use (3.12) to determine the values of V_g and V_ℓ. As we are only interested in one degree of freedom, the generation voltage in the complete system should be equal to the generation voltage in the reduced system; and similarly for the load bus. Namely, separating the terms of (3.12) according to generation and load, we can solve (3.12) with

$$V_g = w_{g1}V_{g1} + w_{g2}V_{g2}, \tag{3.13}$$

$$V_\ell = w_{\ell 1}V_{\ell 1} + w_{\ell 2}V_{\ell 2}, \tag{3.14}$$

where the weights are defined according to (3.1), (3.2), (3.3), and (3.4).

Then the complex voltage difference across the combined transmission lines is

$$V_{g\ell} = V_g - V_\ell. \tag{3.15}$$

If we regard the transmission lines as an area of the power system, then $V_{g\ell}$ is the complex voltage across the area described in (17) (compare (3.13) - (3.15) with (4) of (17)). This approach only depends on the admittances of the lines in the area, and the voltages at the boundaries of the area are combined according to the weights of these admittances. Equations (3.13) and (3.14) combine the voltages of the generation buses and combine the voltages of the load buses, resulting in a reduced system which is a compound of the combination of the voltages, the admittances of the transmission lines that connect the load with the generation, and the sum of the currents in the generation buses and the load buses.

The reduction above applies to the transmission corridor degree of freedom that transfers power from the generators to the loads. If the power network has equal voltages at the generators, and equal voltages at the loads, then only the transmission corridor degree of freedom is

present in the network currents and voltages, and the reduction applies perfectly to the power system. In this case, the contraction of the generator buses into a single bus and the contraction of the load buses into a single bus do not affect the behavior of the network. In particular, the maximum power transfers of the original and reduced networks must be identical.

When the generator voltages differ or the load voltages differ, there are additional degrees of freedom of the network present in the network currents and voltages, and the maximum power transfers of the original and reduced networks can differ. We investigate the impact of this difference on our methods numerically in section 3.1.4.2. In practical high stress cases of interest, we expect that lines with larger susceptances carry larger currents and powers, so that the voltage across the lines can be similar, and the equal voltage conditions at the generators and at the loads can be approximately satisfied.

3.1.4 Results

3.1.4.1 Perfect reduction case

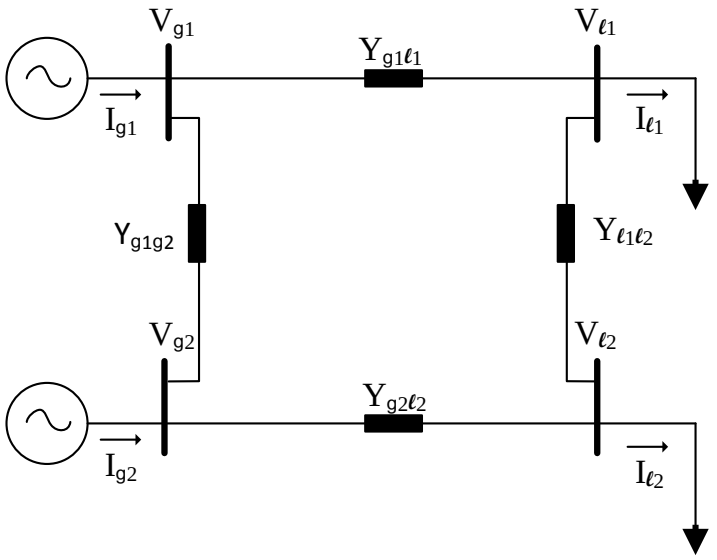

Figure 3.4 Power system with 2 inputs and 2 outputs and 2 lines in corridor.

Table 3.1 Example of perfect reduction

Maximum power transfer of the complete system	
$V_{g1} = 1 + j0$	$V_{g2} = 1 + j0$
$V_{\ell 1} = 0.5 - j0.2$	$V_{\ell 2} = 0.5 - j0.2$
$I_{g1\ell 1} = 6.1 - j8.7$	$I_{g2\ell 2} = 18.4 - j26.1$
$I_{g1g2} = 0$	$I_{\ell 1\ell 2} = 0$
$Y_{g1\ell 1} = 3.8 - j19.1$	$Y_{g2\ell 2} = 11.4 - j57.2$
$Y_{g1g2} = 5.2 - j25.8$	$Y_{\ell 1\ell 2} = 8.2 - j34.8$
$S_{max} = 20 - j12$	
Maximum power transfer of the reduced system	
$w_1 = 0.25$	$w_2 = 0.75$
$V_g = 1 + j0$	$V_\ell = 0.5 - j0.2$
$V_{g\ell} = 0.5 + j0.2$	$I_{g\ell} = 24.5 - j34.8$
$Y_{g\ell} = 15.3 - j76.3$	$Y_\ell = 66.73 - j40.04$
$\mid Y_{g\ell} \mid = 77.82$	$\mid Y_\ell \mid = 77.82$
$S_{g\ell} = 4.6 + j22.8$	$S_\ell = 20 + j12$
$\mid S_{g\ell} \mid = 23.3$	$\mid S_\ell \mid = 23.3$
Index= 100%	

As explained in section 3.1.3, the reduction, and hence the performance of the index, is perfect when the generation voltages are equal and the load voltages are equal. This subsection illustrates this case numerically. We choose equal generation and equal load voltages, shown in Table 3.1, for the four bus system of Fig. 3.4. The values for this power system and its reduction have been adjusted to be at the maximum power voltage collapse condition, and the results in Table 3.1 show that the maximum power transfer is the same for both the complete and reduced systems.

3.1.4.2 General reduction case and numerical assessment of errors

When the generation bus voltages are not equal and/or the load bus voltages are not equal, the maximum transfers of power in the complete and reduced system are not exactly the same, and the index will have an error. This subsection measures this error numerically to help judge its significance. In the four bus system of Fig. 3.4, the generation voltages were assumed to be equal, the load power factor was held constant, and we varied the load voltages by transferring power between the loads. For each set of load voltages, the error in the maximum real load power was assessed using the following steps:

1. Evaluate the maximum transfer of power for the complete system by increasing load powers proportionally.

2. Use the total load power of the complete system as the initial load power in the reduced system.

3. Evaluate the maximum transfer of power for the reduced system by varying the load power.

4. Estimate the error by comparing the maximum total load power of the complete system with the maximum load power of the reduced system.

The results in Table 3.2 show that the error in the maximum transfer of real power exceeds 10% when the difference of the load voltage magnitude exceeds 20%, see Fig. 3.5, and the difference between the voltage angles are more than 13°, see Fig. 3.6.

Table 3.2 Maximum power transfer for a power system with 2 inputs and 2 outputs

Complete system					Reduced system	
$P_{\ell 1}^{\max}$	$P_{\ell 2}^{\max}$	$P_{\ell}^{\max}$	$V_{\ell 1}-V_{\ell 2}$	$\delta_{\ell 1}-\delta_{\ell 2}$	$P_{\ell}^{\max}$	error
9.7	0.0	9.7	-0.3	-19	10.6	-10
9.5	1.1	10.6	-0.29	-18	12.5	-18
9.2	2.3	11.5	-0.28	-18	14.3	-24
9.0	3.8	12.8	-0.26	-17	15.8	-23
8.6	5.7	14.3	-0.24	-16	17.2	-20
8.0	8.0	16	-0.21	-14	18.4	-14
7.7	9.4	17.1	-0.19	-13	19.0	-11
7.2	10.9	18.1	-0.16	-11	19.4	-7
5.9	13.8	19.7	-0.06	-5	19.9	-1
5.0	**14.9**	**19.9**	**0**	**0**	**19.9**	**0**
4	15.8	19.8	-0.05	4	19.9	-1
1.9	17.0	18.9	0.13	10	19.3	-2
0.2	17.8	18	0.17	13	18.3	-2

Angles in degree, error in percent, and all other quantities in per unit.

Perfect reduction case has zero error and is shown in bold face.

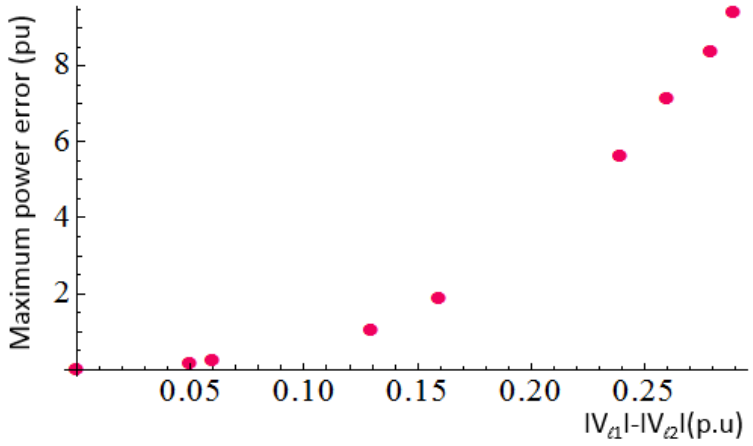

Figure 3.5 Error due to different magnitude voltages

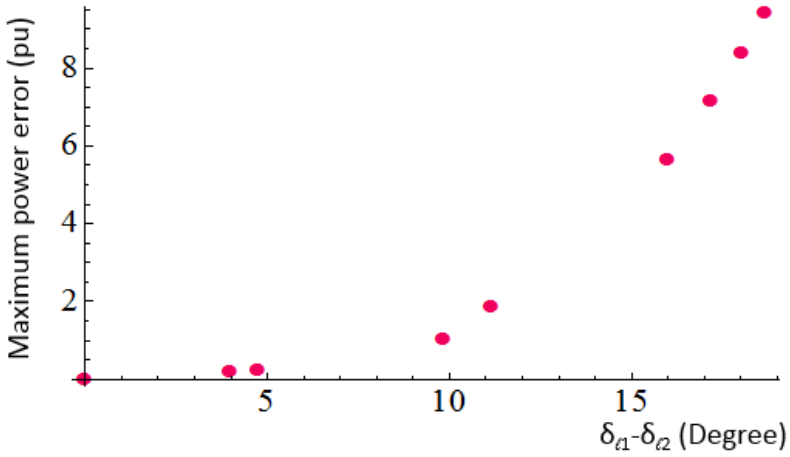

Figure 3.6 Error due to different angle voltages

In practical power systems without contingencies, the load voltage magnitude would vary less than 10% and the difference of the voltage angles would vary less than 10°. This example suggests that the voltage margin index inaccuracy due to the reduction should be less than 10% in the more extreme practical cases, and the inaccuracy due to the reduction would often be much smaller for less extreme cases.

3.1.5 Conclusion

The reduction using the voltage area concept has the effect of reducing multiple transmission lines to a single line equivalent to which on-line voltage stability monitoring with synchrophasor measurements can be applied. The reduction to a single line equivalent is perfect in the special case in which the loads have equal voltages and the generators have equal voltages. That is, in this case, the on-line monitoring of the equivalent single line exactly gives the margin to voltage collapse for the original system. This is a special case, but we studied the general case with a numerical example and found that the errors were reasonably small. Our results suggest that we have found a promising and systematic approach for combining together multiple transmission lines so that single line monitoring methods can be applied.

3.2 Method 2: Complex power conservation reduction

3.2.1 Introduction

The voltage across an area reduction (45), is an initial way for reducing a corridor with multiple lines to an equivalent single line, giving a more justifiable and accurate indication of the margin to voltage collapse. In addition, in this section, we apply a new reduction using synchrophasor measurements, which can give more precise results. This reduction is based on the preservation of the complex power and current of the multiple line system, to the single line system. An initial indication of this reduction was made for for inter-area models for oscillations of large power networks (9).

3.2.2 Reduction

The reduction is analyzed in a 4-bus system with two inputs (generators at bus $g1$ and $g2$) and two outputs (loads at buses $\ell 1$ and $\ell 2$), see Fig. 3.1, that will be reduced to an equivalent system with one input and one output, see Fig. 3.2. The reduction is done specifically in the transmission corridor, which means that the reduction only includes lines. According to this, the four bus system showed in Fig. 3.1, can be represented as Fig. 3.7.

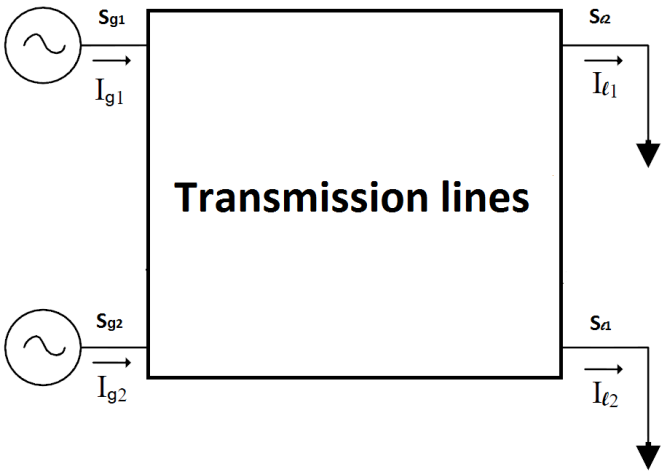

Figure 3.7 Representation of the multiple line transmission corridor

The transmission corridor includes all the lines that are connected the generation area with the load area. The generation area could have loads, but it is mostly generation; in the same way, the load area could have generation but it is mostly loads. The corridor with multiple lines, Fig. 3.7, has complex power and complex current entering to the generation area and leaving the load area. The complex current and voltages (I_{g1} , I_{g2}, $I_{\ell 1}$, $I_{\ell 2}$, V_{g1} , V_{g2}, $V_{\ell 1}$ and $V_{\ell 2}$), are obtained from the PMUs at all the buses that conform the transmission lines corridor.

In this way, the complex power is obtained using the complex currents and voltages measured with the PMUs:

$$S_{g1} = V_{g1} I_{g1}^*, \tag{3.16}$$

$$S_{g2} = V_{g2} I_{g2}^*, \tag{3.17}$$

$$S_{\ell 1} = V_{\ell 1} I_{\ell 1}^*, \tag{3.18}$$

$$S_{\ell 2} = V_{\ell 2} I_{\ell 2}^*. \tag{3.19}$$

The corridor with multiple lines will be reduced to a single line equivalent system preserving the complex power:

$$S_g = S_{g1} + S_{g2}, \tag{3.20}$$

$$S_\ell = S_{\ell 1} + S_{\ell 2}. \tag{3.21}$$

Similarly, the complex current of the multiple line system is equal to the complex current of the equivalent system:

$$I_g = I_{g1} + I_{g2}, \tag{3.22}$$

$$I_\ell = I_{\ell 1} + I_{\ell 2}. \tag{3.23}$$

The voltage of the reduce system is

$$V_g = \frac{S_g}{I_g^*}, \tag{3.24}$$

$$V_\ell = \frac{S_\ell}{I_\ell^*}. \tag{3.25}$$

The voltage across the transmission corridor is defined by:

$$V_{g\ell} = \frac{S_g + S_\ell}{I_g^*}. \tag{3.26}$$

As the transmission corridor has shunt admittance, and assuming that the shunts are equal in both ends of the line, the effect of the shunts in the admittance across the corridor can be modeling in the following way, see (52):

$$Y_{sh} = \frac{I_g - I_\ell}{V_g + V_\ell}, \tag{3.27}$$

$$Y_{g\ell} = \frac{I_g - Y_{sh}V_g}{V_g - V_\ell}. \tag{3.28}$$

Equation (3.28), is also useful in the case that some minor load bus does not have synchrophasor measurements. In this case, (3.28) will correct the current that is absorbing for that load.

3.2.2.1 Relation with voltage across an area reduction

In this subsection, we evaluate the relation between the two method for reducing multiple lines to a single line. We start with method 2, complex power reduction, and use the assumption of method 1, voltage across an area, getting the same results for the weights in both reductions.

We can rewrite (3.24) and (3.25) as

$$V_g = V_g \frac{I_g{}^*}{I_g{}^*}, \tag{3.29}$$

$$V_\ell = V_\ell \frac{I_\ell{}^*}{I_\ell{}^*}. \tag{3.30}$$

According to (3.29) and (3.30), the weights are defined in terms of the currents:

$$w_{gi} = \frac{I_{gi}{}^*}{I_{g\ell}{}^*}. \tag{3.31}$$

The voltage across an area reduction assumes equal voltages at all the generation buses and equal voltages at all the load buses. Hence, using the equal voltages condition at the new equivalent in (3.31), it is possible to get the weights of the voltage across an area reduction:

$$w_{gi} = \frac{I_{gi}{}^*}{I_{g\ell}{}^*} = \frac{(V_{gi}Y_{gi})^*}{(I_{g1} + I_{g2})^*} = \frac{(V_{gi}Y_{gi})^*}{\sum_{i=1}^{n}(V_{gi}Y_{gi})^*}. \tag{3.32}$$

As all the voltages in the generation area are supposed equal, (3.32) is equal to:

$$w_{gi} = \frac{V_g{}^* Y_{gi}{}^*}{V_g{}^* \sum_{i=1}^{n} Y_{gi}{}^*} = \frac{Y_{gi}{}^*}{\sum_{i=1}^{n} Y_{gi}{}^*}. \tag{3.33}$$

Using only the magnitude of the weights, (3.33) is equal to:

$$|w_{gi}| = \left| \frac{Y_{gi}}{\sum_{i=1}^{n} Y_{gi}} \right|. \tag{3.34}$$

Note that (3.34) is similar to (3.1), (3.2), (3.3), and (3.4). Thus, voltage across an area reduction and complex power reduction are equal when voltages are equal in the generation area and equal in the load area.

3.2.3 Assumptions and modeling

In order to locate the bifurcation point of the system, we suppose a stable initial condition and a slowly varying parameters λ, which is the increment of the load power, varying slowly compared with the dynamics of the system. Under those assumptions, the power system can be modeled by the static equations. In addition, the model is based on one slack generation bus, generation buses as PV, and the load buses as PQ.

The objective of this methodology is to determine in real time, how near is the transmission corridor with multiple lines of the bifurcation point under each change of the load. With the

finality of doing it in real time, the system is reduced to a single line where the saddle-node bifurcation is easy to analyze. When the transmission corridor with multiple lines is reduced to a single line system, the generator voltage magnitude $|V_g|$ and the admittance of the single line $Y_{g\ell}$ are converted from variables to constants, which change according to the currents that are circulated in each line of the multiple line system. These variables that are convert to constants in the reduced system will be called $z = \{|V_g|, X_{g\ell}\}$.

However, the voltage stability margin is assuming that z is constant. Thus in order to get the power index which indicates if the multiple line system has voltage stability problems, we need to fix z to its initial value. The initial value is the value that we get from the PMU measurements. To demonstrate that the variation of z does not affect substantially the bifurcation point, we will analyze five cases (A, B, C, and D), see Fig. 3.8.

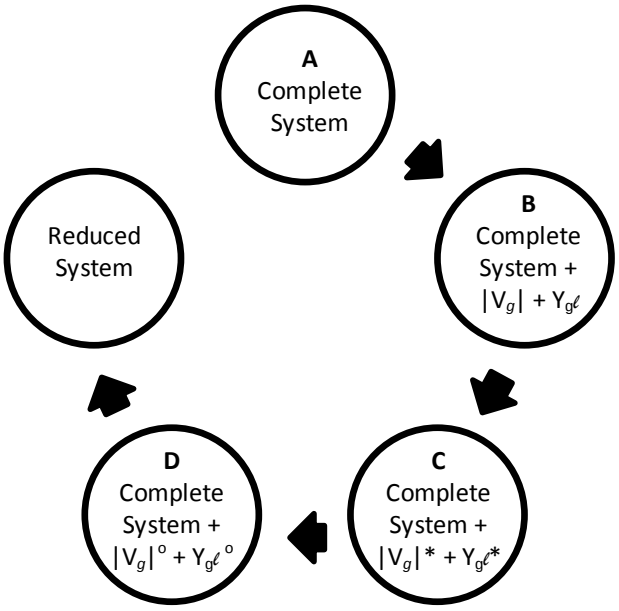

Figure 3.8 Transformation of the multiple line system to the reduce system

For case A, we will evaluate the bifurcation point of the multiple line system. In case B, we will analyze the effect of the z equations on the multiple line system (at this point, the bifurcation is the same, because all the equations go to the instability point at the same time). In addition, for case C, we want to analyze the effect of fixing z at the bifurcation point

and analyze if it has an effect on the bifurcation of the multiple line system. Finally, as was mentioned before, we need to fix z to its initial value, so in case D, we review the change of fixing z at the initial point, for which case we analyzed the sensitivity of this change.

3.2.3.1 Complete system

The static equations of the multiple line system are

$$0 = f_{g1}(x, \lambda) = V_{g1} I_{g1}^* - S_{g1} \tag{3.35}$$

$$0 = f_{g2}(x, \lambda) = V_{g2} I_{g2}^* - S_{g2} \tag{3.36}$$

$$0 = f_{\ell 1}(x, \lambda) = V_{\ell 1} I_{\ell 1}^* - S_{\ell 1} \tag{3.37}$$

$$0 = f_{\ell 2}(x, \lambda) = V_{\ell 2} I_{\ell 2}^* - S_{\ell 2} \tag{3.38}$$

The state is $x = (\delta_{g2}, |V_{\ell 1}|, |V_{\ell 2}|, \delta_{\ell 1}, \delta_{\ell 2})$, and the parameter is λ. Loads 1 and 2 are PQ loads, generator 2 is PV and generator 1 is a slack bus. $y = (\delta_{g1}, |V_{g1}|, |V_{g2}|)$ are constants.

The currents $I_{g1}, I_{g2}, I_{\ell 1}, I_{\ell 2}$ are function of the state variables x and the parameter λ. Moreover, the complex load powers are functions of λ:

$$S_{\ell 1} = P_{\ell 1}(\lambda) + jQ_{\ell 1}(\lambda) = P_{\ell 1}^o + \lambda + j(Q_{\ell 1}^o + k\lambda) \tag{3.39}$$

$$S_{\ell 2} = P_{\ell 2}(\lambda) + jQ_{\ell 2}(\lambda) = P_{\ell 2}^o + \lambda + j(Q_{\ell 2}^o + k\lambda) \tag{3.40}$$

In addition, $S_{g1} = P_{g1} + jQ_{g1}$ and $Q_{g2} = \mathrm{Im}\{S_{g2}\}$ are functions of λ because they increase as required by the load increase and power balance. The case A equations are summarized as

$$0 = f(x, \lambda) \tag{3.41}$$

The bifurcating equilibrium of (3.41) is at (x_*, λ_*).

3.2.3.2 Multiple line system plus the z variables

Case B is obtained from case A by adding extra equations $0 = g(x, z, \lambda)$ that include the extra variables $z = (|V_g|, \delta_g, \mathrm{Re}\{Y_{g\ell}\}, \mathrm{Im}\{Y_{g\ell}\})$, and we modified the conventional power flow

equations (3.36), (3.37), and (3.38) in order to include the new variables.

$$0 = f_{g2}(x, z, \lambda) = V_g I_{g1}^* + V_g I_{g2}^* - V_{g1} I_{g1}^* - S_{g2} \tag{3.42}$$

$$0 = f_{\ell 1}(x, z, \lambda) = \frac{|I_{g1} + I_{g2}|}{Y_{g\ell}} - V_g I_{g1}^* - V_g I_{g2}^* - V_{\ell 2} I_{\ell 2}^* - S_{\ell 1} \tag{3.43}$$

$$0 = f_{\ell 2}(x, z, \lambda) = \frac{|I_{g1} + I_{g2}|}{Y_{g\ell}} - V_g I_{g1}^* - V_g I_{g2}^* - V_{\ell 1} I_{\ell 1}^* - S_{\ell 2} \tag{3.44}$$

$$0 = g_{V_g}(x, z, \lambda) = \frac{S_{g1} + S_{g2}}{I_{g1}^* + I_{g2}^*} - V_g \tag{3.45}$$

$$0 = g_{Y_{g\ell}}(x, z, \lambda) = \frac{I_{g1} + I_{g2}}{\frac{S_{g1}+S_{g2}}{(I_{g1}+I_{g2})^*} - \frac{S_{\ell 1}+S_{\ell 2}}{(I_{\ell 1}+I_{\ell 2})^*}} - Y_{g\ell} \tag{3.46}$$

V_g is the voltage at the generation side of the reduced system and $Y_{g\ell}$ is the equivalent complex admittance of the reduced system.

The augmented state is $X = (x, z) = (\delta_{g2}, |V_{\ell 1}|, |V_{\ell 2}|, \delta_{\ell 1}, \delta_{\ell 2}, |V_g|, \delta_g, \mathrm{Re}\{Y_{g\ell}\}, \mathrm{Im}\{Y_{g\ell}\})$. Note that setting equations (3.45) and (3.46) to zero allows the z variables to be calculated from the original state variables x.

The case B equations are summarized as

$$\begin{aligned} 0 &= f(x, \lambda) \\ 0 &= g(x, z, \lambda) \end{aligned} \tag{3.47}$$

The bifurcating equilibrium of (3.47) is at (x_*, z_*, λ_*). There is an exact correspondence between solutions x of (3.41) in case A and solutions (x, z) of (3.47) in case B. In particular, case B bifurcates with a saddle-node bifurcation exactly when case A bifurcates[1]. That is, adding the z variables and their equations has no effect on the bifurcation.

3.2.3.3 Multiple line system plus the z variables fixed to their values at the bifurcation

Case C is obtained from case B by fixing the z variables to their values z_* at the bifurcation, and eliminating (3.45) and (3.46). That is, variables z become constant z_*. V_{g_*} and $Y_{g\ell_*}$ are constants, which are the values of V_g and $Y_{g\ell}$ at the bifurcation. In this way, the constant are $Y = (V_{g1}, V_{g2}, \delta_{g1}, V_{g_*}, Y_{g\ell_*})$.

[1]Saddle-node bifurcation generically occurs when two static solutions coincide; for details see (16)

Equations (3.42), (3.43) and (3.44) become

$$0 = f_{g2}(x,\lambda) = V_{g_*} I^*_{g1} + V_{g_*} I^*_{g2} - V_{g1} I^*_{g1} - S_{g2} \tag{3.48}$$

$$0 = f_{\ell 1}(x,\lambda) = \frac{|I_{g1} + I_{g2}|}{Y_{g\ell_*}} - V_{g_*} I^*_{g1} - V_{g_*} I^*_{g2} - V_{\ell 2} I^*_{\ell 2} - S_{\ell 1} \tag{3.49}$$

$$0 = f_{\ell 2}(x,\lambda) = \frac{|I_{g1} + I_{g2}|}{Y_{g\ell_*}} - V_{g_*} I^*_{g1} - V_{g_*} I^*_{g2} - V_{\ell 1} I^*_{\ell 1} - S_{\ell 2} \tag{3.50}$$

The case C equations are summarized as

$$0 = f(x,\lambda) \tag{3.51}$$

Recalling that (3.47) has a bifurcating equilibrium at (x_*, z_*, λ_*), it is clear that (3.51) still has an equilibrium (x_*, λ_*). However, the change from variables z to parameters z_* changes the system Jacobian, and at the equilibrium (x_*, z_*, λ_*). Equation (3.51) generally has a nonsingular Jacobian and is generally not bifurcating. For case C, the state is x, the constant is $Y = \{y, z_*\}$ and the parameters is λ.

3.2.3.4 Multiple line system plus the z variables fixed to their values at the operating point

Case D is obtained from case C by changing the value of the z parameters from z_* to z_0, the value of z at the operating point. Ecuations (3.48), (3.49) and (3.50) become

$$0 = f_{g2}(x,\lambda) = V_{g0} I^*_{g1} + V_{g0} I^*_{g2} - V_{g1} I^*_{g1} - S_{g2} \tag{3.52}$$

$$0 = f_{\ell 1}(x,\lambda) = \frac{|I_{g1} + I_{g2}|}{Y_{g\ell_0}} - V_{g_0} I^*_{g1} - V_{g0} I^*_{g2} - V_{\ell 2} I^*_{\ell 2} - S_{\ell 1} \tag{3.53}$$

$$0 = f_{\ell 2}(x,\lambda) = \frac{|I_{g1} + I_{g2}|}{Y_{g\ell_0}} - V_{g_0} I^*_{g1} - V_{g0} I^*_{g2} - V_{\ell 1} I^*_{\ell 1} - S_{\ell 2} \tag{3.54}$$

Where V_{g0} , $Y_{g\ell_0}$ are constants, which values are corresponding to the initial point. For case D, the state is x, the constant is $Y = \{y, z_0\}$ and the parameters is λ. The case D equations are summarized as

$$0 = f(x,\lambda) \tag{3.55}$$

3.2.3.5 Reduced system

Finally, for the reduced system is considered the power flow equations, assuming the generator bus as slack, and the load bus as PQ. The generator voltage and the admittance are set at the initial point of the multiple line system.

The static equation of the reduced system is

$$h_g(x_r, \lambda_r) = V_g I_g^* - S_g \tag{3.56}$$

$$h_\ell(x_r, \lambda_r) = V_\ell I_\ell^* - S_\ell \tag{3.57}$$

The state is $x_r = (|V_\ell|, \delta_\ell)$, and the parameter is λ_r, where P_g, Q_g, P_ℓ, and Q_ℓ are function of λ_r:

$$P_\ell(\lambda_r) = P_\ell^o + \lambda_r = (P_{\ell 1}^o + P_{\ell 2}^o) + 2\lambda \tag{3.58}$$

$$Q_\ell(\lambda_r) = Q_\ell^o + k\lambda_r = (Q_{\ell 1}^o + Q_{\ell 2}^o) + 2k\lambda \tag{3.59}$$

3.2.4 Results

As mentioned before, using continuation power flow it is possible to calculate the bifurcation point of the reduced system under a specified pattern of load increase. It is almost the same as the pattern of load increase for the complete system. In order to illustrate the similarity between the bifurcations of the reduced system and the complete system, we analyze the system shown in Fig. 3.4. For each case we analyze the bifurcation point, and find the maximum load that the system can supply, see Table 3.3. As was mentioned, fixing z almost does not affect the bifurcation point, and the results in all the cases are almost the same, which allows us to fix z in the reduced system, without any problems. With this example, we demonstrate numerically that to fix the variable z does not affect significantly the maximum transfer of the corridor.

Table 3.3 Comparison of the bifurcation of the reduced system and the complete system

Case	Description	Maximum power
A	Complete system	15.76 - j 9.5
B	Complete System plus equations of the reduced system	15.76 - j 9.5
C	Complete System plus equations of the reduced system at bifurcation point	15.76 - j 9.5
D	Complete System plus equations of the reduced system at initial point	15.79 - j 9.5
E	Reduce system	15.79 - j 9.5

Quantities in per unit.

3.2.5 Conclusion

In this section, we indicate a new method for reducing multiple transmission lines to a single line equivalent to which on-line voltage stability monitoring with synchrophasor measurements can be applied. This method preserves the complex power and complex current of the original system. In addition, this reduction accounts for transfer of power between generation and between loads. This makes the model more accurate in extreme cases such as line trips and generation trips. In addition, this reduction is exactly equal to voltage across an area reduction in the specific case where voltage are equal in generation, and equal in load.

CHAPTER 4. COMPARISON BETWEEN THE REI EQUIVALENT AND THE PROPOSED REDUCTIONS

4.1 Introduction

Chapter 3, presented two reductions that can be used for online voltage stability assessments. The first one uses the new concept voltage across an area, and the second uses the conservation of complex power. In this chapter, we compare the voltage across an area reduction and complex power reduction techniques with older network equivalent derivations and in particular the REI (Radial Equivalent Independent) equivalent proposed by (13).

It is important to clarify that this chapter is part of joint work in collaboration with Professor Costas Vournas from National Technical University of Athens. The comparison was initiated by him, the section about REI equivalent was written by him. Since he gave an interpretation of the area angle and independently also suggested a power reduction, we decided to collaborate.

4.2 Two-bus equivalent formulation

The equivalents are analyzed in a four bus system with two sending buses $s1$, $s2$, and two receiving buses $r1$ and $r2$, see Fig. 4.1, that will be reduced to an equivalent system with one sending bus and one receiving bus. However, it is easy to generalize this to an n bus system. For all three equivalents, the total current into the transmission corridor is preserved:

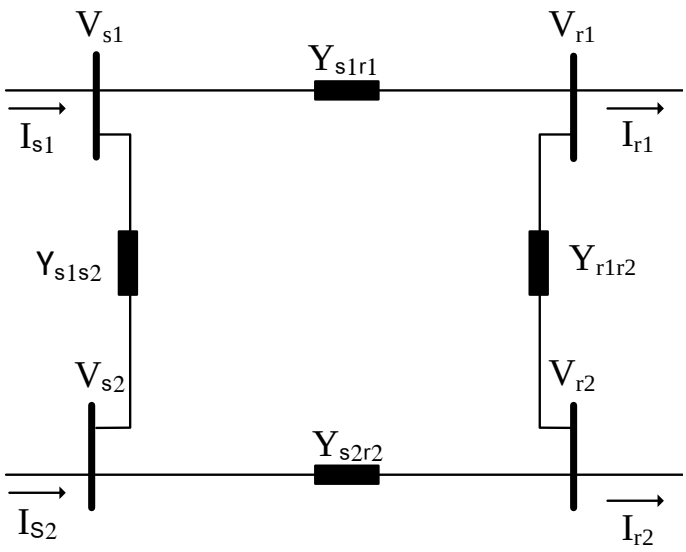

Figure 4.1 Corridor definition

$$I_S = \sum_{i=1}^{n} I_{si} \tag{4.1}$$

$$I_R = \sum_{i=1}^{n} I_{ri} \tag{4.2}$$

$$I_S = -I_R. \tag{4.3}$$

4.2.1 The REI equivalent

The REI equivalent is an extension of the well-known Ward equivalent (3), (54). The main idea of the REI equivalent is to transform all loads and generation of the "external network" into equivalent shunt admittances to ground and then introduce a REI bus connected to the ground bus through an admittance equal to the negative of the sum of shunt admittances. For summing of all the shunt admittance, the REI equivalent assumes equal voltage for the sending buses, and equal voltages for the receiving buses. For the corridor shown in Fig. 4.1 the REI equivalent, see Fig. 4.2, is described by the following equations:

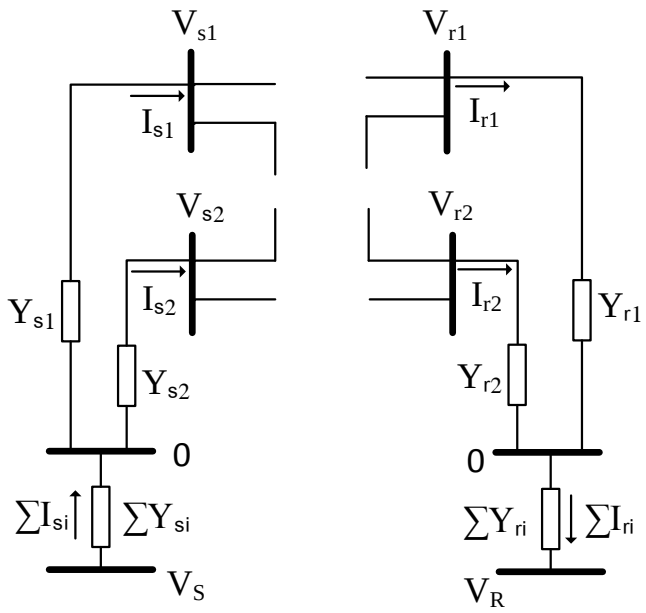

Figure 4.2 Introduction of REI buses

$$Y_{si} = \frac{I_{si}}{V_{si}}, \tag{4.4}$$

$$Y_{ri} = \frac{I_{ri}}{V_{ri}}, \tag{4.5}$$

$$V_S = \frac{I_S}{\sum_{i=1}^{n} Y_{si}}, \tag{4.6}$$

$$V_R = \frac{I_R}{\sum_{i=1}^{n} Y_{ri}}, \tag{4.7}$$

$$Y_S = \frac{I_S}{V_S - V_R}. \tag{4.8}$$

In addition, the REI equivalent can do a internal reduction, as described in (4.8). For the external reduction, it should be noted that the ground bus of Fig. 4.2 cannot be eliminated using Gauss formula as the diagonal element is by definition equal to zero. Thus, the ground bus has to be eliminated with admittances directly connected between the REI bus and the sending (resp. receiving) buses defined, see Fig. 4.3, so that the injected current is maintained in the equivalent:

$$Y_{Si} = \frac{I_{si}}{V_S - V_{si}}, \tag{4.9}$$

$$Y_{Ri} = \frac{I_{ri}}{V_{ri} - V_R}. \tag{4.10}$$

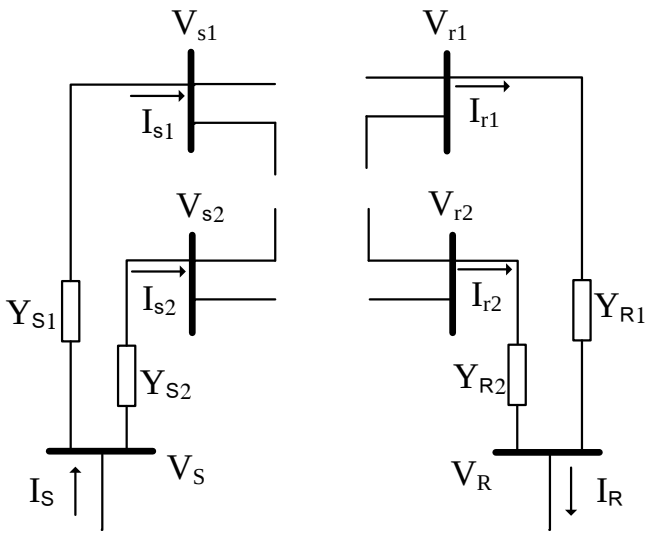

Figure 4.3 REI equivalent

4.2.2 Voltage across an area equivalent

The main idea of the voltage across an area equivalent, (17), (45), is to combine all admittance of the internal network in an equivalent admittance and combine the voltages of the sending/receiving with the weights of the lines (w_{siri}). As the REI equivalent, it is assuming equal voltage for the sending buses, and equal voltages for the receiving buses. For the corridor shown in Fig. 4.1 the voltage across an are equivalent is described by the following equations:

$$Y_S = \sum_{i=1}^{n} Y_{siri}, \tag{4.11}$$

$$w_{siri} = \frac{Y_{siri}}{\sum_{i=1}^{n} Y_{siri}}, \tag{4.12}$$

$$V_S = \sum_{i=1}^{n} w_{siri} * V_{si}, \tag{4.13}$$

$$V_R = \sum_{i=1}^{n} w_{siri} * V_{ri}. \tag{4.14}$$

4.2.3 Complex power equivalent

The representation of the complete system will be reduced to a single line equivalent system using the conservation of power law, where the transmission corridor has the same amount of complex power entering and leaving it as the equivalent system. In other words, all the power

that is going in/out of the "internal network" is equal to all the power that going in/out of the equivalent system.

For the corridor shown in Fig. 4.1 the complex power equivalent is described by the following equations:

$$S_{si} = V_{si} {I_{si}}^*, \tag{4.15}$$

$$S_{ri} = V_{ri} {I_{ri}}^*, \tag{4.16}$$

$$S_S = \sum_{i=1}^{n} S_{si}, \tag{4.17}$$

$$S_R = \sum_{i=1}^{n} S_{ri}, \tag{4.18}$$

$$V_S = \frac{S_S}{{I_S}^*}, \tag{4.19}$$

$$V_R = \frac{S_R}{{I_R}^*}, \tag{4.20}$$

$$Y_S = \frac{I_S}{V_S - V_R}. \tag{4.21}$$

4.3 Comparison of the three equivalents

For the system shown in Fig. 4.1, we develop the three equivalents, and we get similar results for the voltage magnitude and angle, see Table 4.1. However, we get different results of the impedance, because for the REI equivalent and voltage across an area equivalents we assumed equal voltages between sending buses, and between receiving buses.

4.4 Conclusion

It is advantageous to reduce several lines to a single line, which can be applicable in different fields of power system as voltage stability, and power markets, real time monitoring. It is important to clarify that the three reduction are preserving different properties of the corridor, and these correspond to different assumptions.

All the equivalents are preserving the current of the complete system. The REI equivalent can be used for external, and internal reduction, while the voltage across an area and the complex power reduction only can do internal reduction. Furthermore, the complex power

Table 4.1 Comparison of the three equivalents

Corridor Data

$V_{s1} = 1 + j0$	$V_{s2} = 1 - j0.87$	$V_{r1} = 0.95 - j0.09$
$V_{r2} = 0.93 - j0.13$	$I_{s1} = -4.16 + j0.29$	$I_{s2} = -0.69 + j3.56$
$I_{r1} = 0.49 - j0.36$	$I_{r2} = 4.36 - j3.48$	$Y_{s1r1} = 3.8 - j19.1$
$Y_{s2r2} = 11.5 - j57.3$	$Y_{s1s2} = 5.2 - j25.9$	$Y_{r1r2} = 8.2 - j34.8$

Two-bus Equivalent of Transmission Corridors

Equivalent	$\|V_S\|$	δ_S	$\|V_R\|$	δ_R	Y_S
REI	0.969	-0.039	0.942	-0.13	19.18+ j 65.21
Voltage across an area	0.999	-0.065	0.944	-0.124	15.26- j 76.31
Complex power	1.03	-0.039	0.942	-0.13	9.67 - j 47.70
Thevenin load 1	1	0.013	0.942	-0.13	9.67 - j 47.70

Angles in radians, and all other quantities in per unit.

equivalent is preserving the complex power and the admittance of the corridor. According to all the assumptions, the three equivalents are exactly equal under the condition of equal voltages at the sending buses and equal voltages at the receiving buses because in this case all satisfy the assumption.

CHAPTER 5. NEW INDEX FOR EVALUATING VOLTAGE STABILITY MARGIN ONLINE

5.1 Introduction

After reducing the corridor with multiple lines to a single bus system it is possible to evaluate the voltage stability margin on the single line system. The most used voltage stability indexes that can be found in the literature for a single line are the Thévenin index (53), and VSLBI index (38). However, we found that those indexes are not linear with respect to the loading margin, and they are not easy to understand for operators in a control center room. Thus, in this chapter, we propose a new index which is based on the maximum real power that the corridor can transfer.

5.2 Voltage stability index formulation

5.2.1 VSLBI derivation

At the beginning of this work, we used the VSLBI voltage stability index, which is based on the fact that the maximum transfer of power occurs when the voltage magnitude of the load bus is equal to the voltage magnitude drop in the transmission corridor impedance (38), so that

$$VSLBI = \frac{|V_\ell|100}{|V_{g\ell}|} \tag{5.1}$$

To understand better the VSLBI index, we start with the assumption that we have two buses, one as slack ($\delta_g = 0$) with constant voltage magnitude, the other as PQ. Using the fact that the current flowing across the line is equal to the current that is feeding the load, one way to

derive the voltage stability index shown in (5.1) is

$$\frac{(V_g - V_\ell)^*}{Z_{g\ell}{}^*} = \frac{S_\ell}{V_\ell} \tag{5.2}$$

Rewriting (5.2), we have:

$$V_\ell (V_g - V_\ell)^* = S_\ell Z_{g\ell}{}^*. \tag{5.3}$$

For a given S_ℓ, we have a specific $Z_{g\ell}$, and V_g. Hence $Z_{g\ell}$, and V_g are fixed at one specific load demand. According by (5.3) has two solutions for V_ℓ:

$$V_\ell = V_\ell{}^{(1)}, \tag{5.4}$$

$$V_\ell = V_\ell{}^{(2)} = (V_g - V_\ell{}^{(1)})^*. \tag{5.5}$$

From (5.4), and (5.5):

$$V_\ell = V_\ell{}^{(2)}, \tag{5.6}$$

$$V_\ell = (V_g - V_\ell{}^{(2)})^* = (V_g - (V_g - V_\ell{}^{(1)})^*)^* = V_g{}^* - V_g + V_\ell{}^{(1)}. \tag{5.7}$$

At the bifurcation point, the two solutions coalesce to one. Hence (5.4) must be equal to (5.7):

$$V_\ell{}^{(1)} = (|V_g| \angle - \delta_g) - (|V_g| \angle \delta_g) + V_\ell{}^{(1)}. \tag{5.8}$$

Rewriting (5.8), we get:

$$(|V_g| \angle - \delta_g) = (|V_g| \angle \delta_g). \tag{5.9}$$

As $\delta_g = 0$, the equality in (5.9) is satisfied. At this point, we have proved that with the assumptions we get only one solution at the bifurcation. Now we can state the index, using the fact that in the bifurcation $V_\ell = V_\ell{}^{(1)} = V_\ell{}^{(2)}$, then (5.5) can be write as:

$$V_\ell = (V_g - V_\ell)^*, \tag{5.10}$$

$$|V_\ell| = |V_{g\ell}|\,. \tag{5.11}$$

According to this we can get the index shown in (5.1).

As the VSLBI index is based on a fraction of voltage, it is nonlinear. It is difficult to state how far the transmission corridor is from the instability point.

5.2.2 New voltage stability index derivation

In order to have one index that can linearly describe how far the corridor with multiple lines is to the voltage instability, we introduce a new index which is tracking the maximum power that the corridor can transport. For the VSLBI index, we are assuming the generation bus as PV, the load bus as PQ, a constant power factor, constant generator voltage magnitude, and constant equivalent admittance between the generation and load.

Now we derive the new voltage stability index. First, we combining the complex current of the transmission corridor $I_{g\ell}$, and the complex power at the load S_ℓ:

$$P_\ell + jQ_\ell = \frac{V_g V_\ell \angle(\delta_g - \delta_\ell) - V_\ell^2}{R_{g\ell} + jX_{g\ell}}. \tag{5.12}$$

After algebraic manipulation, (5.12) can be express as:

$$V_\ell^4 + (2R_{g\ell}P_\ell + 2X_{g\ell}Q_\ell - V_g^2)V_\ell^2 + (P_\ell^2 + Q_\ell^2)(R_{g\ell}^2 + X_{g\ell}^2) = 0. \tag{5.13}$$

Solving (5.13), and using the fact that at the bifurcation point of (5.13) has only one solution, we have:

$$(2R_{g\ell}P_\ell + 2X_{g\ell}Q_\ell - V_g^2)^2 - 4((P_\ell^2 + Q_\ell^2)(R_{g\ell}^2 + X_{g\ell}^2)) = 0. \tag{5.14}$$

Doing algebraic manipulations, and assuming constant power factor ϕ in (5.14), the maximum load power of a single line system is

$$P_{max} = \frac{-V_g^2 R_{g\ell} - V_{g\ell}^2 X_{g\ell}\tan\phi + \sqrt{V_g^4(1+\tan^2\phi)(R_{g\ell}^2 + X_{g\ell}^2)}}{2(X_{g\ell} - R_{g\ell}\tan\phi)^2}. \tag{5.15}$$

Using the maximum load power of (5.15), the voltage stability index is

$$Index = \frac{P_\ell 100}{P_{max}}. \tag{5.16}$$

An alarm can be triggered when a sufficient percentage of the maximum power across the reduction system is exceeded. For example, the alarm could be triggered when the index exceeds 60%.

5.3 Comparison of the VSLBI index and the new maximum power index

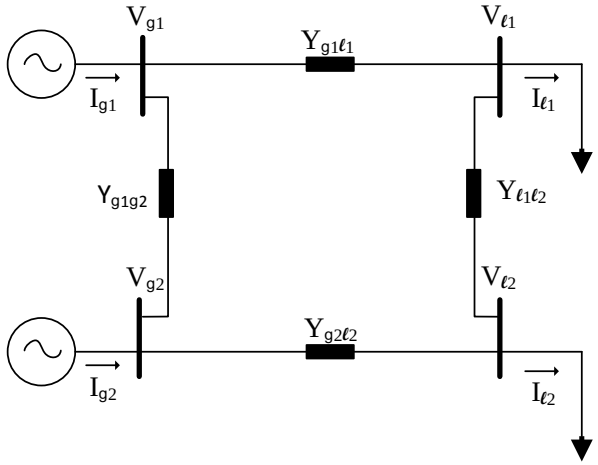

Figure 5.1 Power system with 2 inputs and 2 outputs and 2 lines in corridor.

Table 5.1 Comparison of the three equivalents

Corridor Data

$V_{g1} = 1 + j0$	$V_{g2} = 0.96 - j0.27$	$V_{\ell 1} = 0.62 - j0.22$
$V_{\ell 2} = 0.43 - j0.33$	$I_{g1} = -12.88 + j5.92$	$I_{g2} = -2.13 + j29.8$
$I_{\ell 1} = 0.66 - j0.81$	$I_{\ell 2} = 14.35 - j34.9$	$Y_{g1\ell 1} = 3.8 - j19.1$
$Y_{g2\ell 2} = 11.5 - j57.3$	$Y_{g1g2} = 5.2 - j25.9$	$Y_{\ell 1\ell 2} = 8.2 - j34.8$

Two-bus Equivalent of Transmission Corridors

Equivalent	VSLBI	New Index
Voltage across area	87.3	93
Complex power	110.3	99.7

Angles in radians, index in percentage, and all other quantities in per unit.

In this section, we compare the VSLBI voltage stability index, and the new index proposed in (5.16). For comparing the two voltage stability indexes, we apply them in the four bus system of Fig. 5.1, for different combination of loads. For each combination of load, we comparing the results of both indexes with the maximum transfer of power according to the continuation power flow.

5.3.1 Numerical assessment of the margin error using VSBLI and the new index for voltage across area and complex power reduction method

The objective is to compare the voltage stability margin of the complete system of Fig. 5.1 and its reduced system. First we evaluate the maximum load of the complete system using a continuation power flow. After that, using the data for the complete system, we reduce the system and get its margin.

Clearly, the voltage stability margin using voltage across the reduction is an excellent estimate under the assumption of equal voltages at the generation and equal voltage at the loads. However, as was mentioned before, under different voltages we can have an error in the voltage stability index. The error using the VSLBI index is less than 60%, see Fig. 5.2, and it can be reduced to less than 40% using the new index, see Fig. 5.3.

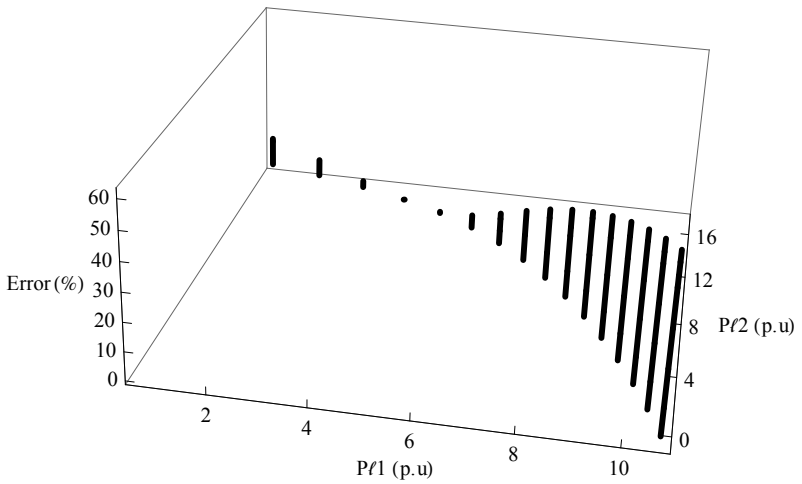

Figure 5.2 Error index for different combinations of power load using the voltage across area reduction - VSLBI Index

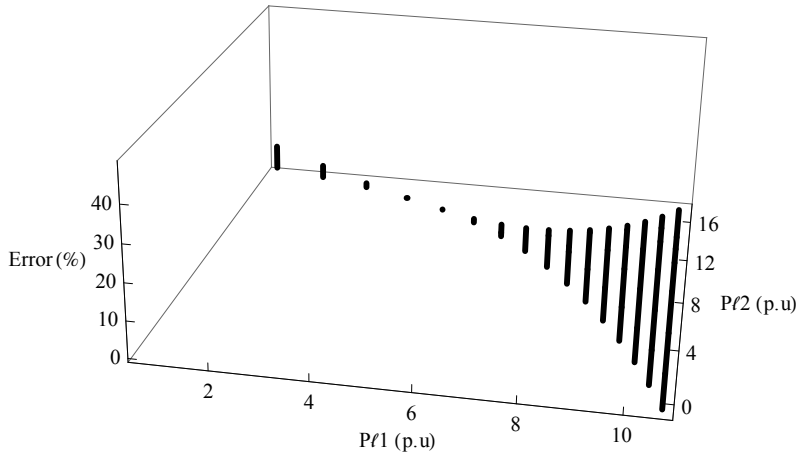

Figure 5.3 Error index for different combinations of power load using the voltage across area reduction - maximum power index

The margin using complex power reduction is a good estimate of the voltage stability margin. There is a small error, which is due to the variation of the reduce voltage magnitude V_g, and the equivalent admittance $Y_{g\ell}$, which are considered constant in the voltage stability margin proposed in (5.16). For the most extreme cases the maximum error using the complex power reduction and VSBLI index was less than 15%, see Fig. 5.4, and using the new index the error was less than 0.8%, see Fig. 5.5.

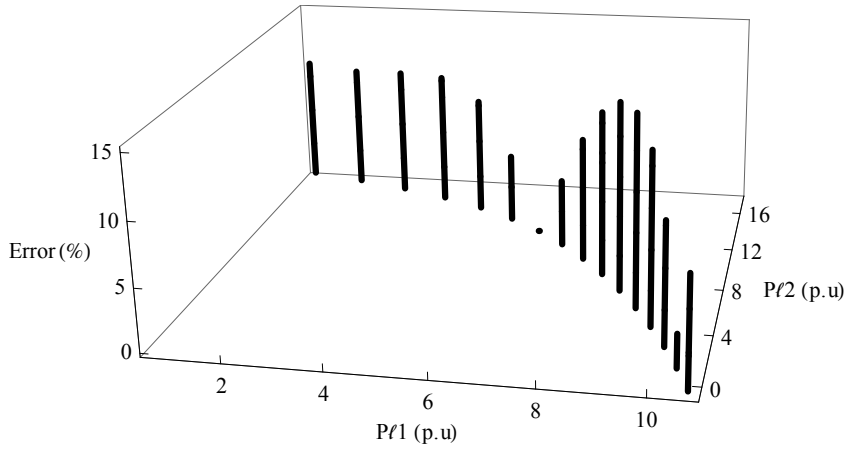

Figure 5.4 Error index for different combinations of power load using the complex Power reduction - VSLBI Index

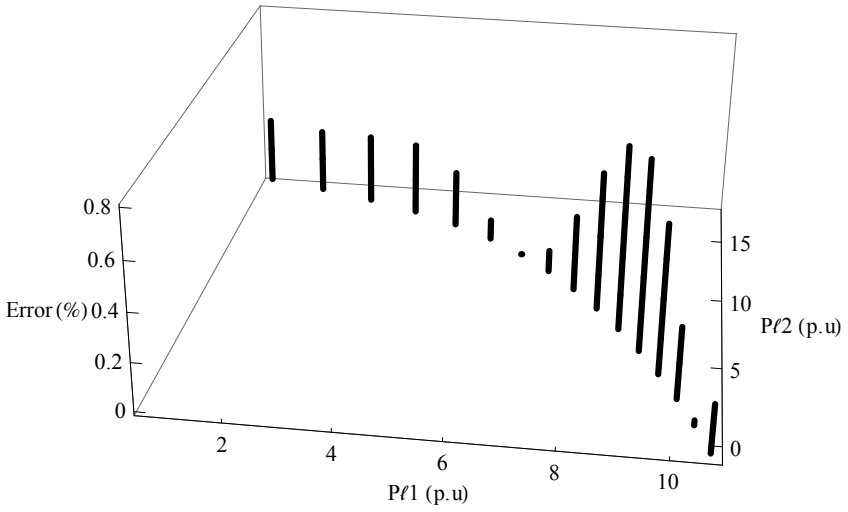

Figure 5.5 Error index for different combinations of power load using the complex Power reduction - maximum power index

5.4 Conclusion

It is advantageous to track the voltage stability margin using the maximum load that can be transferred to the corridor with multiple lines. According to the results the maximum power index is a good estimate, and it has the advantage of being in terms of a quantity that it is commonly used and monitored in control centers. From the results, we can see how the index error is reduced from 60% to 0.8%, using the complex power reduction, and the new maximum power index. Thus, these new methods show an excellent approximation, and performance for predicting the voltage stability margin of the transmission corridor with multiple lines.

CHAPTER 6. METHODOLOGY FOR ONLINE EVALUATION OF VOLTAGE STABILITY INDEX OF MULTIPLE LINES SYSTEMS USING SYNCHROPHASOR MEASUREMENTS

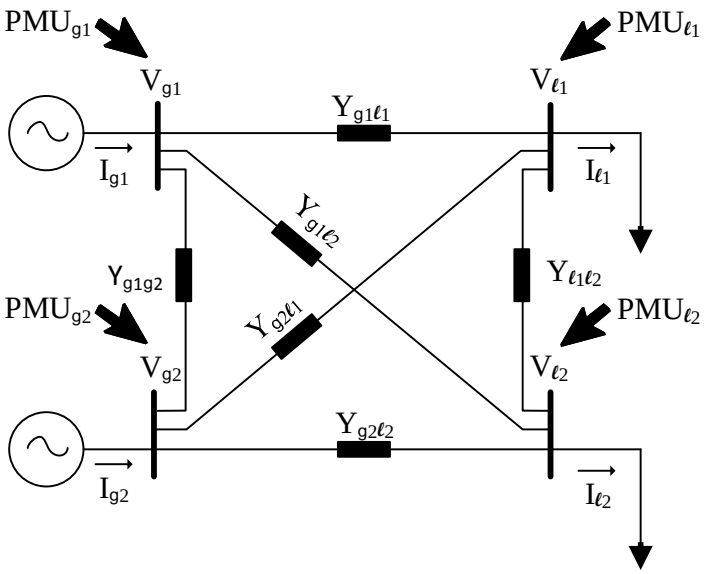

Figure 6.1 Power system with 2 inputs and 2 outputs and 4 lines in corridor.

In Chapter 3, was shown two new methods for reducing multiple transmission lines to a single line. We want to reduce the corridor with multiple lines to a single line to find a way of measuring the voltage stability margin online. To do this, we will use synchrophasor measurements, the reductions, and the power voltage stability index.

6.1 Combining measurements - voltage across an area reduction

For evaluating voltage stability online using the voltage across an area reduction and synchrophasor measurements, we require the following steps for a four bus system with two inputs

and two outputs, see Fig. 6.1. The same method can be applying to an n bus system by a simple elaboration of notation:

1. Measure the complex voltage and current at both ends of all the transmission lines in the corridor, see Fig. 6.1.

2. Use the synchrophasor measurements to find the admittance of each transmission line, and the equivalent admittance:

$$Y_{g1\ell1} = \frac{I_{g1\ell1}}{V_{g1} - V_{\ell1}}, \tag{6.1}$$

$$Y_{g1\ell2} = \frac{I_{g1\ell2}}{V_{g1} - V_{\ell2}}, \tag{6.2}$$

$$Y_{g2\ell1} = \frac{I_{g2\ell1}}{V_{g2} - V_{\ell1}}, \tag{6.3}$$

$$Y_{g2\ell2} = \frac{I_{g2\ell2}}{V_{g2} - V_{\ell2}}, \tag{6.4}$$

$$Y_{g\ell} = Y_{g1\ell1} + Y_{g1\ell2} + Y_{g2\ell1} + Y_{g2\ell2}. \tag{6.5}$$

3. Use the admittance to find the weight of each bus:

$$w_{g1} = \frac{Y_{g1\ell1} + Y_{g1\ell2}}{Y_{g\ell}}, \tag{6.6}$$

$$w_{g2} = \frac{Y_{g2\ell1} + Y_{g2\ell2}}{Y_{g\ell}}, \tag{6.7}$$

$$w_{\ell1} = \frac{Y_{g1\ell1} + Y_{g2\ell1}}{Y_{g\ell}}, \tag{6.8}$$

$$w_{\ell2} = \frac{Y_{g1\ell2} + Y_{g2\ell2}}{Y_{g\ell}}. \tag{6.9}$$

4. Combine the voltages using the weights into the equivalent voltage for the generation and load area:

$$V_g = w_{g1}V_{g1} + w_{g2}V_{g2}, \tag{6.10}$$

$$V_\ell = w_{\ell1}V_{\ell1} + w_{\ell2}V_{\ell2}. \tag{6.11}$$

5. Evaluate the voltage stability index:

$$Index = \frac{P_\ell 100}{P_{max}}, \tag{6.12}$$

where:

$$P_{max} = \frac{-V_g^2 R_{g\ell} - V_{g\ell}^2 X_{g\ell} \tan\phi + \sqrt{V_g^4(1+\tan^2\phi)(R_{g\ell}^2 + X_{g\ell}^2)}}{2(X_{g\ell} - R_{g\ell}\tan\phi)^2}. \tag{6.13}$$

6.2 Combining measurements - complex power reduction

For evaluating voltage stability online using the complex power reduction and synchrophasor measurements, we require the following steps for a four bus system with two inputs and two outputs. The steps are the same for an n bus system:

1. Measure with a PMU the complex voltage and current at both ends of all the transmission lines that connect the generation area with the load area, see Fig. 6.1.

2. Use the synchrophasor measurements to find the complex power of the generation area and the load area:

$$S_g = V_{g1} {I_{g1}}^* + V_{g2} {I_{g2}}^*, \tag{6.14}$$

$$S_{ell} = V_{\ell 1} {I_{\ell 1}}^* + V_{\ell 2} {I_{\ell 2}}^*. \tag{6.15}$$

3. Combine the complex current into the equivalent line current:

$$I_{g\ell} = I_{g1} + I_{g2}. \tag{6.16}$$

4. Using the complex power of each area and the current across the transmission corridor to find the voltages of the reduced system:

$$V_g = \frac{S_g}{{I_{g1} + I_{g2}}^*}, \tag{6.17}$$

$$V_\ell = \frac{S_\ell}{{I_{\ell 1} + I_{\ell 2}}^*}. \tag{6.18}$$

5. Using the complex voltage and complex currents of each area to find the admittance of the reduced system:

$$Y_{sh} = \frac{I_g - I_\ell}{V_g + V_\ell}, \tag{6.19}$$

$$Y_{g\ell} = \frac{I_g - Y_{sh} V_g}{V_g - V_\ell}. \tag{6.20}$$

6. Evaluate the voltage stability index:

$$Index = \frac{P_\ell 100}{P_{max}}, \tag{6.21}$$

where:

$$P_{max} = \frac{-V_g^2 R_{g\ell} - V_{g\ell}^2 X_{g\ell} \tan\phi + \sqrt{V_g^4 (1 + \tan^2\phi)(R_{g\ell}^2 + X_{g\ell}^2)}}{2(X_{g\ell} - R_{g\ell} \tan\phi)^2}. \tag{6.22}$$

6.2.1 Complex power reduction for the WSCC 9 bus and IEEE 39 bus test systems

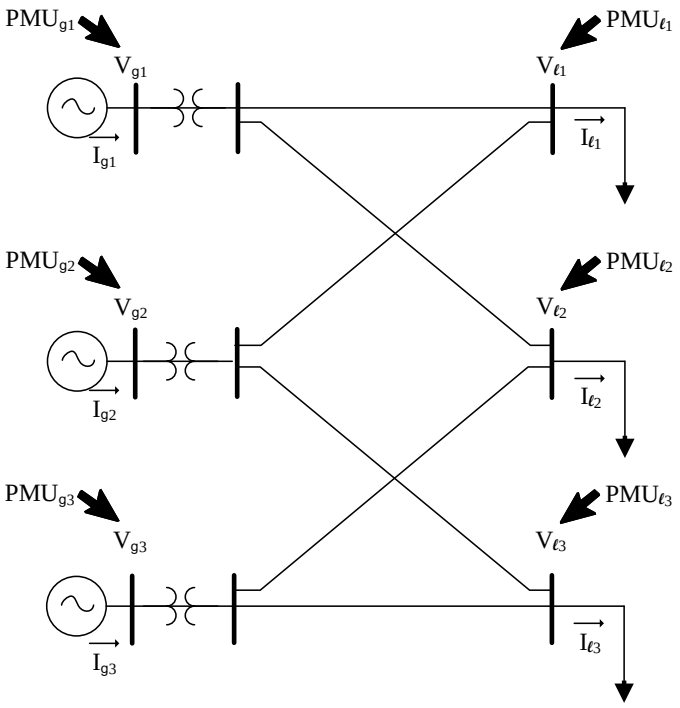

Figure 6.2 WSCC 9 bus test system

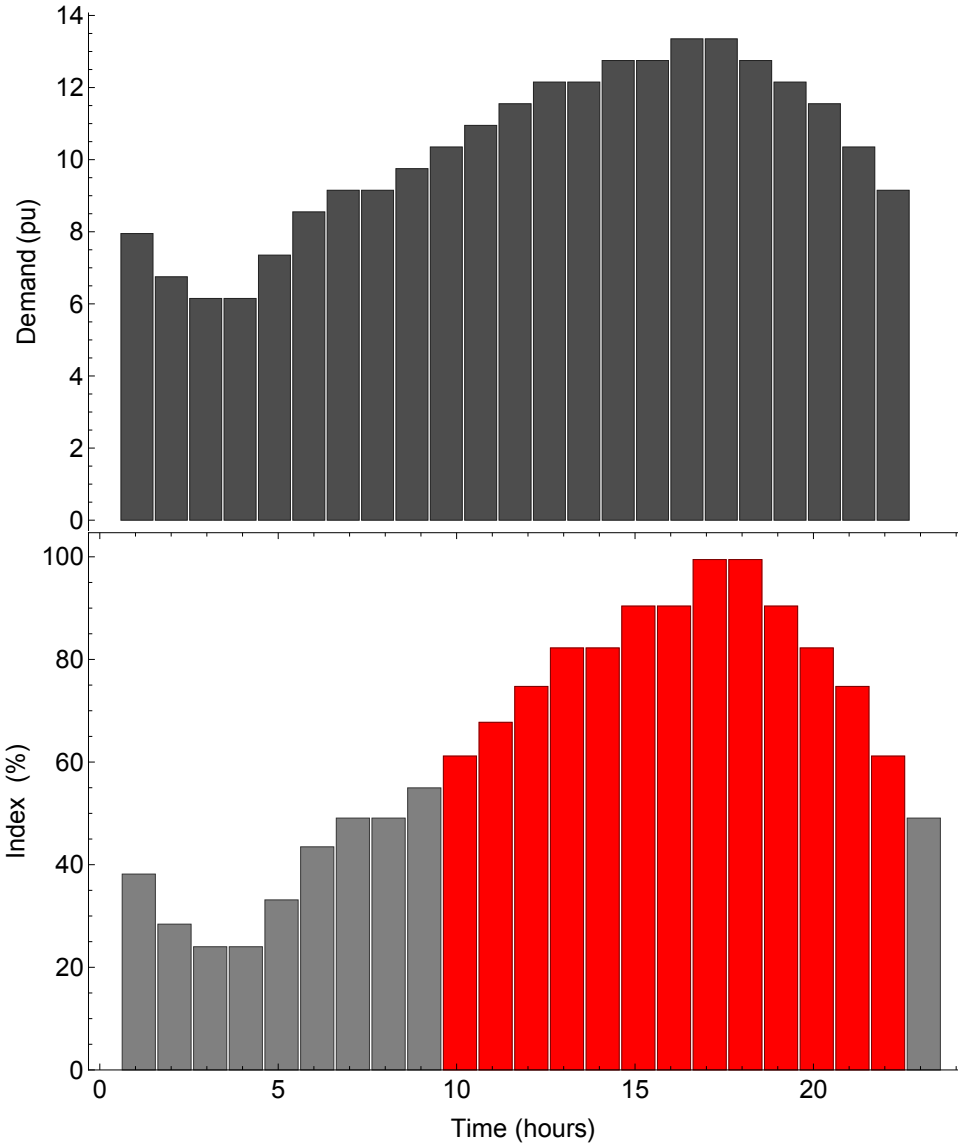

Figure 6.3 Load duration curve and voltage stability margin for the WSCC 9 bus test system

The complex power reduction and the new index are tested in the WSCC 9 bus test system and IEEE 39 bus test system. For the WSCC 9 bus system, the corridor is formed for all the buses and lines of the system, see Fig. 6.2. For the IEEE 39 bus system, the corridor is formed by the generation buses 33, 34, 35, and 36, and for the load buses 16, 20, 21, 23, and 24, see Fig. 6.4.

For those systems, we define a load duration curve for the 24 hours of the day, and after

that, we apply the complex power reduction and power index for each hour. The results for both systems show that the voltage stability index is tracking the stress of the system, and as the load increases the voltage stability margin decreases, see Fig. 6.3 and Fig. 6.5.

Those results are a practical way to show the severity of the power transfer between areas. Currently, it is very important due to the intermittence sources as wind and solar, where the power systems are expose to power flow changes in the order of few minutes. In this way the operator can modify the power flows in real time keeping the voltage stability margen in the secure limits.

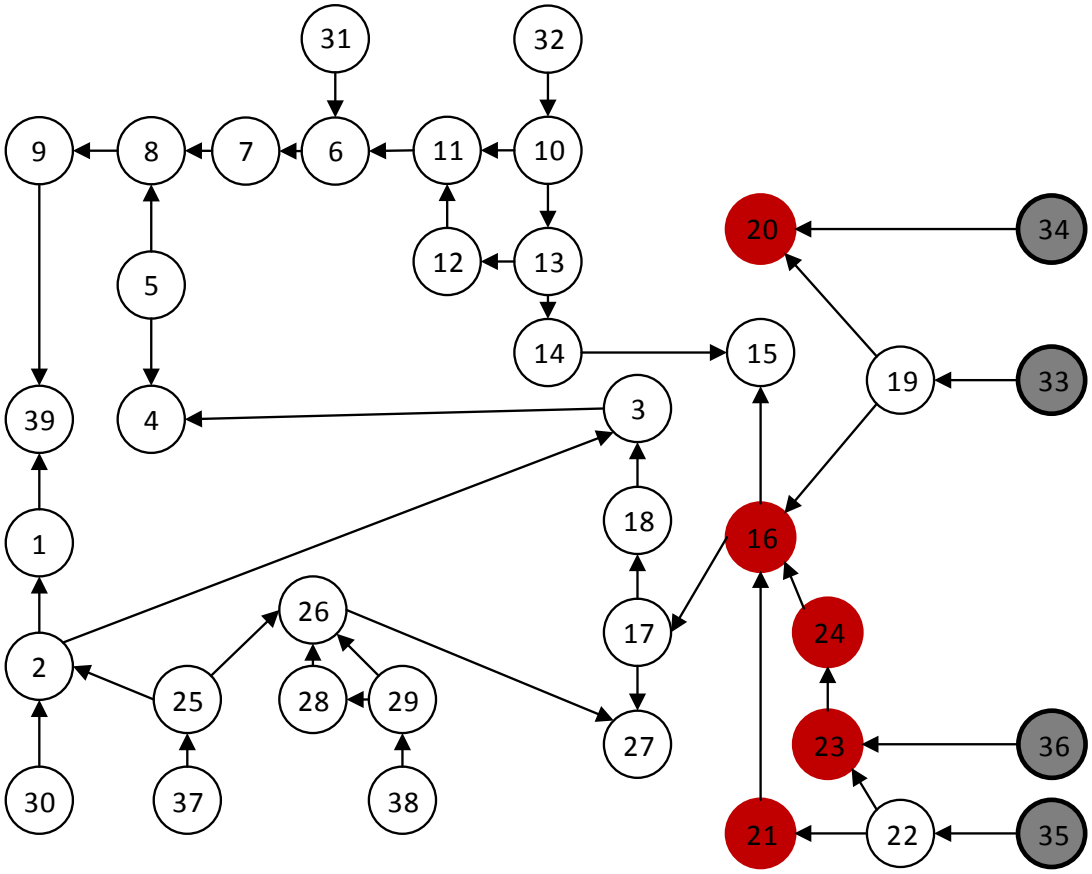

Figure 6.4 IEEE 39 bus test system

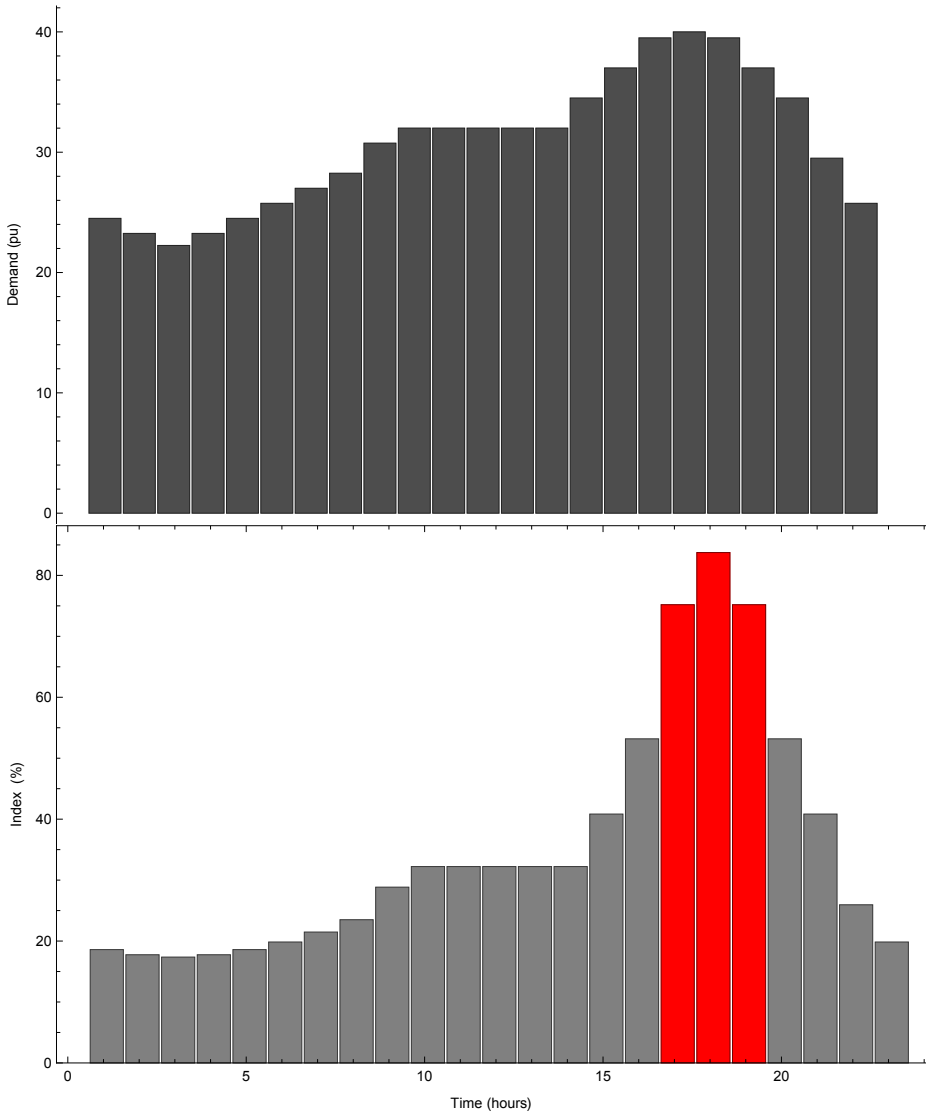

Figure 6.5 Load duration curve and voltage stability margin for the IEEE 39 bus test system

6.3 Generator reactive power limits

In this section, we analyze the effect of the generator reactive power limits using the complex power reduction. In the literature, we can find some previous approaches to include the reactive limits in models for evaluating voltage stability online (19), (24), (38). The foremost reason for analyzing reactive limits is that the bifurcation and its margin can change drastically when

a generator bus that is a PV bus changes to a PQ bus. In case that a generator reaches its reactive limits, the methodology presented in Section 6.2 includes the generator bus as a load bus. For example, in case that the bus g2 of the system showed in Fig. 6.1 reach its reactive limits, the methodology for evaluating the voltage stability index would be

1. Measure with a PMU the complex voltage and current at both ends of all the transmission lines that connect the generation area with the load area, see Fig. 6.1.

2. Check the reactive power limit signal of the generation buses. In the case that the generator reaches its reactive power limit, then it will be considered as a load bus. For example, in this case we suppose that bus g_2 reaches its reactive power limit.

3. Use the synchrophasor measurements to find the complex power of the generation area and the load area, where the generation bus that change to a load bus is treated as a negative load:

$$S_g = S_{g1} = V_{g1} {I_{g1}}^*, \tag{6.23}$$

$$S_\ell = S_{\ell 1} + S_{\ell 2} - S_{g2} = V_{\ell 1} {I_{\ell 1}}^* + V_{\ell 2} {I_{\ell 2}}^* - V_{g2} {I_{g2}}^*. \tag{6.24}$$

4. Combine the complex current into the equivalent line current:

$$I_g = I_{g1}, \tag{6.25}$$

$$I_\ell = I_{\ell 1} + I_{\ell 2} - I_{g2}. \tag{6.26}$$

5. Use the complex power of each area and the current across the transmission corridor to find the voltages of the reduce system:

$$V_g = \frac{S_g}{{I_g}^*}, \tag{6.27}$$

$$V_\ell = \frac{S_\ell}{{I_\ell}^*}. \tag{6.28}$$

.

6. Use the complex voltage, and complex currents of each area for finding the admittance of the reduced system:

$$Y_{sh} = \frac{I_g - I_\ell}{V_g + V_\ell}, \tag{6.29}$$

$$Y_{g\ell} = \frac{I_g - Y_{sh}V_g}{V_g - V_\ell}. \tag{6.30}$$

7. Evaluate the voltage stability index:

$$Index = \frac{P_\ell 100}{P_{max}}, \tag{6.31}$$

where:

$$P_{max} = \frac{-V_g^2 R_{g\ell} - V_{g\ell}^2 X_{g\ell}\tan\phi + \sqrt{V_g^4(1+\tan^2\phi)(R_{g\ell}^2 + X_{g\ell}^2)}}{2(X_{g\ell} - R_{g\ell}\tan\phi)^2}. \tag{6.32}$$

For illustration, we analyze the system of Fig. 6.1 without reactive limits, see Table 6.1, and the same system with a reactive limit of 1.2 p.u in the generator 2, see Table 6.2. As expected, with only this modification the maximum transfer of the load of the system is reduced to 33% in comparison with the case where the generator 2 does not have reactive limits.

6.4 Conclusion

This chapter presented two new methodologies for evaluating online voltage stability for corridors with multiple lines. These methodologies are based on synchrophasor measurements, which give the advantage over current methodologies of having the voltage stability margin in real time without doing simulation, and without using the state estimator, and it is totally independent of the topology data. In addition, we present how to proceed when a generator of the multiple lines corridor reach its reactive limits, which is necessary to apply the methodology to real cases. The complex power reduction, and the complex index were tested in the WSCC 9 bus test system, and in one corridor of the IEEE 39 bus system. The voltage stability margin tracked the load duration curve in both of these systems.

Table 6.1 Maximum transfer of power without reactive limits.

Complete system			
$V_{g1} = 1 + j0$	$V_{g2} = 0.9 - j0.4$	$V_{\ell 1} = 0.4 - j0.3$	$V_{\ell 2} = 0.6 - j0.4$
$I_{g1} = -17.7 + j9.9$	$I_{g2} = 4.9 + j18.3$	$I_{\ell 1} = 7.3 - j17.6$	$I_{ell2} = 5.5 + j10.63$
$S_{g1} = -17 + j9.9$	$S_{g2} = -2 - j18.9$	$S_{\ell 1} = 8.4 + j5$	$S_{\ell 2} = 7.4 + j4.4$
Index= 100%			

Reduced System	
$V_g = 1.1 + j0.2$	$\mid V_g \mid = 19.7$
$V_\ell = 0.49 - j0.34$	$\mid V_\ell \mid = 18.4$
$S_g = 16.5 + j26.8$	
$S_\ell = -15.8 - j9.5$	
Index= 107%	

Table 6.2 Maximum transfer of power including reactive limits

Complete system			
$V_{g1} = 1 + j0$	$V_{g2} = 0.69 - j0.11$	$V_{\ell 1} = 0.53 - j0.21$	$V_{\ell 2} = 0.51 - j0.2$
$I_{g1} = -10.7 + j15.5$	$I_{g2} = -2.5 + j2.2$	$I_{\ell 1} = 5.9 - j7.9$	$I_{\ell 2} = 7.2 - j9.8$
$S_{g1} = -10.7 - j15.5$	$S_{g2} = -2 - j1.2$	$S_{\ell 1} = 4.8 - j2.9$	$S_{\ell 2} = 5.8 + j3.5$
Index= 100%			

Reduced System	
$V_g = 1 + j0$	$V_\ell = 0.48 - j0.2$
$I_g = -10.7 + j15.5$	$I_\ell = 10.7 - 15.5$
$S_g = -10.7 - j15.5$	$S_\ell = 8.6 + j5.2$
Index= 105%	

CHAPTER 7. APPLYING OF THE VOLTAGE STABILITY INDEX FOR MULTIPLE CONTINGENCIES

7.1 Introduction

Voltage collapse under n-1 contingency can be assessed based on power flow analysis and the state estimator (40),(20),(30),(29), (21). However, it takes some time, and there is scope for quickly monitoring multiple outages based on synchrophasor measurements. In addition, multiple outages are prone to occur during bad weather or cyber-physical attacks. However, for reasons of cost and computational time, multiple contingencies cannot be systematically addressed in a real power system (50). For this reason, we address online operational advice about the voltage margin for multiple contingencies in transmission corridors that are connecting areas. Namely, we propose a complementary methodology for evaluating online the contingencies that are not covered under pre-contingency n-1 analysis, giving awareness and recommending control center actions to remedy the problems of voltage stability under the more extreme contingencies.

For evaluating the voltage collapse margin under contingencies, we reduce multiple lines of transmission corridors to a single line using synchrophasor measurements of complex power and current at each end of each line in the transmission corridor. A transmission corridor with multiple lines is reduced to a single line while preserving the complex power and currents entering and leaving the corridors. Then the new voltage stability index can be applied. Hence, this chapter presents how the combined synchrophasor measurements can be used to measure the voltage collapse margin online under unusual increments of load, line outages, or generation outages.

Our method is tested in WSCC 9-bus test system, IEEE 25 bus system, and a real voltage

collapse event in an area of the Colombian system. For each system, we first reduce the multiple line system to a single line system using synchrophasor measurements. Then, we show the voltage collapse margin without contingencies for each system, and then for multiple contingencies until the systems collapse. For the WSCC 9 bus system, we found the voltage collapse margin using our PMUs methodology, and using MATPOWER and VSAT, getting similar results to those well-known voltage stability softwares. In addition, the application of the methodology proposed in this chapter to the real voltage collapse event of the Colombian system, supports the effectiveness of the methodology for tracking the voltage collapse margin under multiple contingencies.

7.2 Summary of the methodology for evaluating online voltage collapse margin across a transmission corridor with multiple contingencies

Considering the assumption and condition presented in Chapter 6, the methodology for evaluation online voltage collapse margin across transmission corridors with multiple contingencies for the system shown in Fig 7.1 is:

1. Select the corridor that can have voltage stability problems according to operational issues or problems that can be identified during the planning process, see Fig. 7.1. For example in case that the planning process identifies that some areas transfer a lot of power to a load area, and under voltage stability simulation of n-2 or more contingencies the system can present voltage stability problems, it can be a good candidate corridor for the online voltage stability evaluation using the PMU method. After selecting the corridor, divide the corridor in generation and load areas, see Fig. 7.1.

2. Measure with PMUs the complex voltage and current at both ends of all the transmission lines that connect the generation area with the load area, see Fig. 7.1.

3. Check the reactive power limit signal of the generation buses. In case that the generator bus reaches its reactive limit then the bus is considered as a load.

4. Use the synchrophasor measurements to find the complex power of the generation area and the load area.

$$S_g = \sum_{i=1}^{n} S_{gi} \tag{7.1}$$

$$S_\ell = \sum_{i=1}^{n} S_{\ell i}. \tag{7.2}$$

5. Combine the complex current into the equivalent single line current:

$$I_g = \sum_{i=1}^{n} I_{gi}, \tag{7.3}$$

$$I_\ell = \sum_{i=1}^{n} I_{\ell i}. \tag{7.4}$$

6. Using the complex power of each area and the current to find the voltages of the reduced system:

$$V_g = \frac{S_g}{I_g{}^*}, \tag{7.5}$$

$$V_\ell = \frac{S_\ell}{I_\ell{}^*}, \tag{7.6}$$

$$V_{g\ell} = \frac{S_g + S_\ell}{I_g{}^*}. \tag{7.7}$$

7. Find the equivalent admittance of the single line, see Eq. (7.9).

$$Y_{sh} = \frac{I_g - I_\ell}{V_g + V_\ell}, \tag{7.8}$$

$$Y_{g\ell} = \frac{I_g - Y_{sh}V_g}{V_g - V_\ell}. \tag{7.9}$$

8. Evaluate the voltage stability index:

$$Index = \frac{P_\ell 100}{P_{max}}, \tag{7.10}$$

where P_{max} is the approximate maximum power that the corridor can transfer, and ϕ is the power factor of the load:

$$P_{max} = \frac{-R_{g\ell}V_g^2 - Tan^2\phi V_{g\ell}^2 X_{g\ell} + \sqrt{V_g^4(1+tan^2\phi)(R_{g\ell}^2 + X_{g\ell}^2)^2}}{2(-Tan\phi R_{g\ell} + X_{g\ell})^2}. \tag{7.11}$$

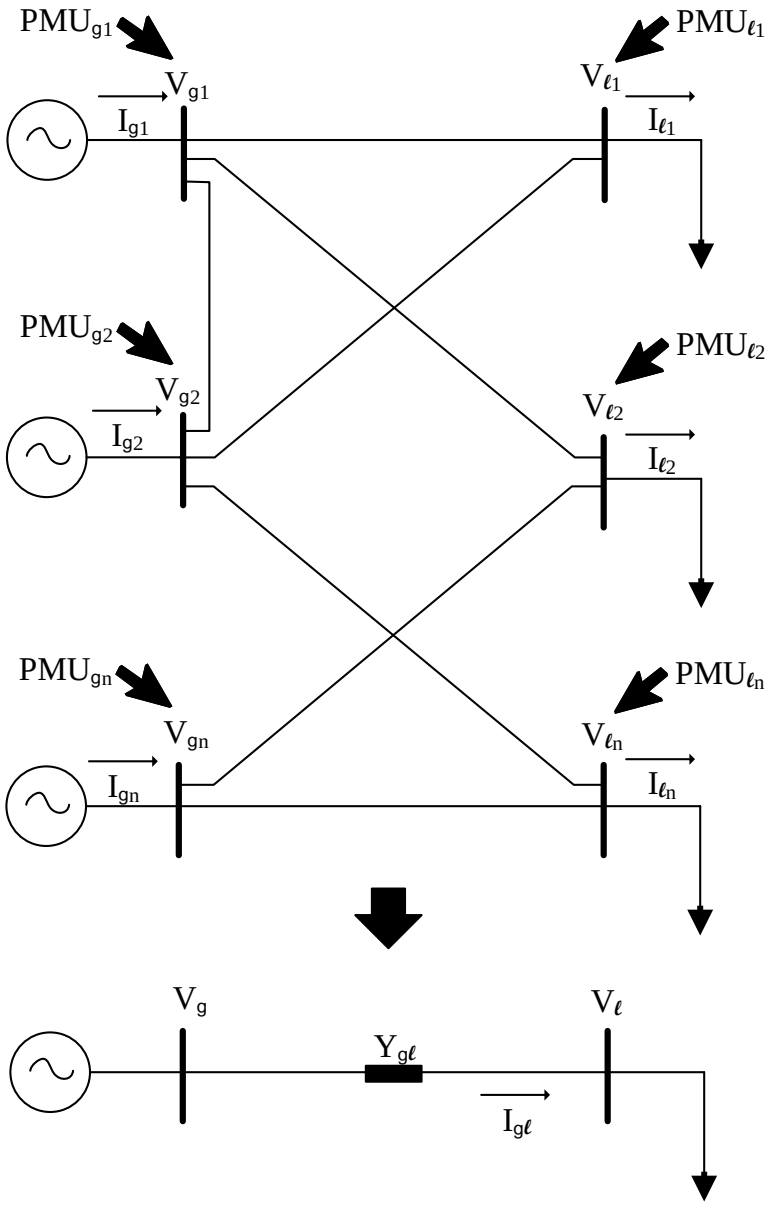

Figure 7.1 Reduction of a power system with n-inputs and n-outputs to a single line system

7.3 Results

7.3.1 Comparison of the online voltage stability margin with MATPOWER, and VSAT for the WSCC 9 bus system

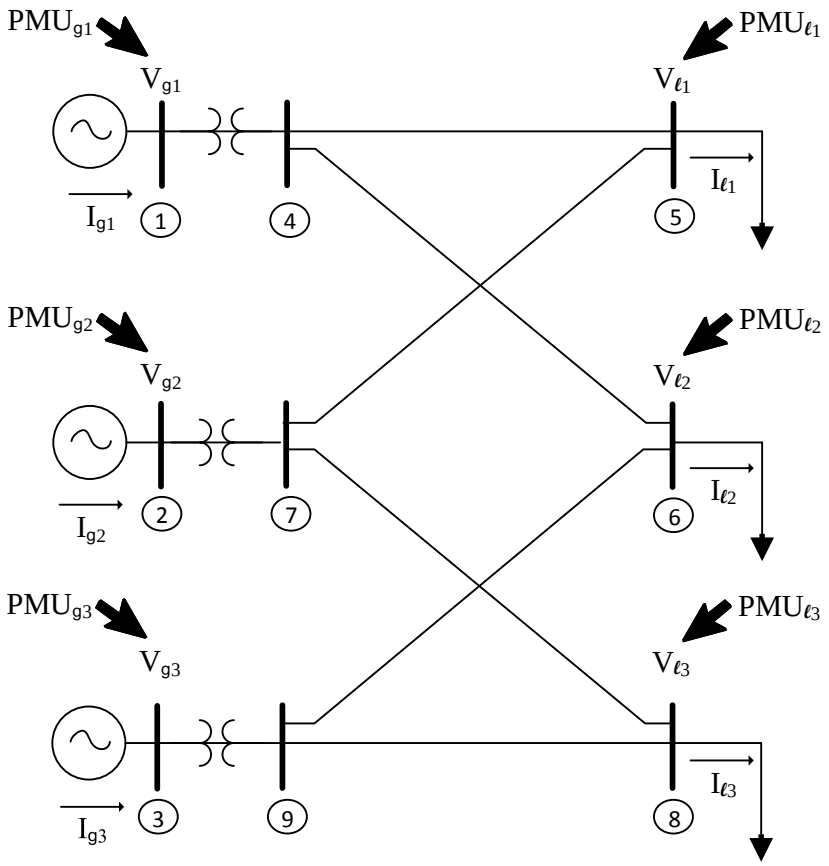

Figure 7.2 WSCC 9-bus test system corridors with three inputs and three outputs

We study the WSCC 9-bus test system shown in Fig. 7.2. We divide this system into two areas, the generation area and the load area. Each area is composed of three buses, and the areas are connected by six lines which form the transmission corridor. This system requires six PMUs to measure the complex voltage and current in all six buses bounding the transmission corridor.

In order to explain better the reduction, we first evaluate the voltage stability margin of the WSCC 9-bus test system without a contingency, see Table 7.1. For this, we measure with the

PMUs the complex voltage and currents in all the buses bounding the transmission corridor, and calculate the complex power entering or leaving at each bus. Combining the complex powers and current for the generation and load areas, we obtain the equivalent voltage for each area, reducing the transmission corridor to a single line system to which we apply the voltage stability index.

Table 7.1 Reduction of WSCC 9-bus system and its voltage stability margin

Multiple line system		
$V_{g1} = 0.99 + j0.4$	$V_{g2} = 0.99 + j0.16$	$V_{g3} = 1 + j0.08$
$V_{\ell 1} = 0.95 - j0.07$	$V_{\ell 2} = 0.97 - j0.07$	$V_{\ell 3} = 0.99 + j0.01$
$I_{g1} = 0.72 - j0.24$	$I_{g2} = 1.63 + j0.13$	$I_{g3} = 0.84 + j0.1$
$I_{\ell 1} = 1.26 - j0.62$	$I_{\ell 2} = 0.9 - j0.4$	$I_{\ell 3} = 1.02 - j0.34$
Reduce System		
$I_g = 3.2 - j0.004$	$I_\ell = 3.18 - j1.34$	
$S_g = 3.2 + j0.35$	$S_\ell = 3.15 + j1.15$	
$V_g = 1 + j0.11$	$V_\ell = 0.97 - j0.05$	
$Y_{sh} = 0.03 + j0.67$	$Y_{g\ell} = -0.31 - j21$	
$P_{\ell max} = 7.53$	$Index = 42\%$	

Values in p.u

In order to show that the results are accurate, we compare our voltage stability margin results for the WSCC 9-bus test system case that we show in Table 7.1 against MATPOWER Version 5.1, and VSAT Version 13.

MATPOWER is a package of MATLAB M-files that can solve a continuation power flow, giving as result the maximum load that the system can supply before the voltage instability point (59). The results for the the WSCC 9-bus test system case using MATPOWER are shown in Table 7.2, and the PV curve of the load 3 is shown in Fig. 7.3. For running the simulation

it was assumed that all the loads increase at the same time and in the same proportion. The results show that the maximum load of the WSCC 9-bus system without contingency is 7.1 p.u, and the voltage collapse margin is 44%. In this way, the method that we propose differ 2% from the continuation power flow results, which is an excellent result for the PMU voltage collapse tool.

Table 7.2 Maximum load of the WSCC 9-bus system using Matpower

$V_{\ell 1}$	$V_{\ell 2}$	$V_{\ell 3}$	$P_{\ell max}$	$Index$
0.633	0.702	0.838	7.1	44%

Values in p.u.

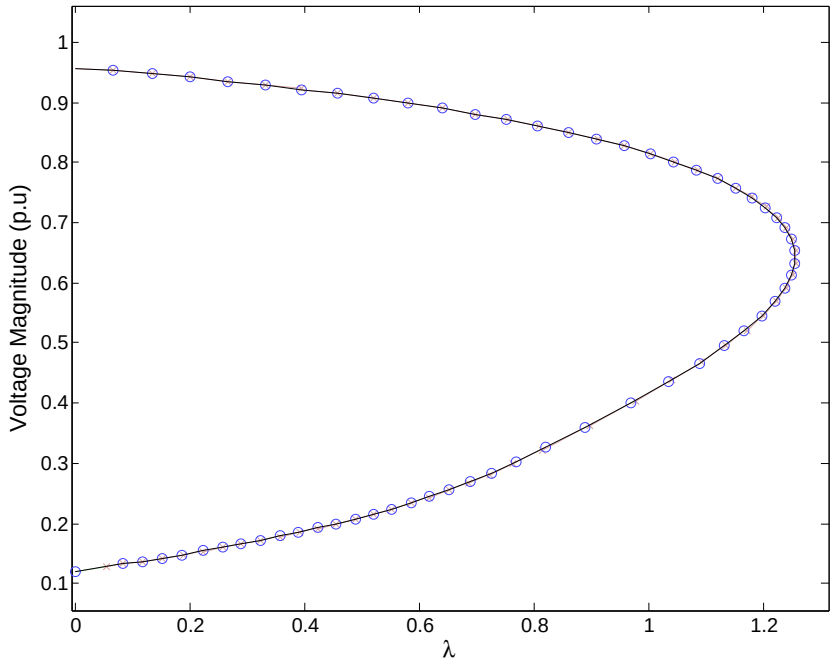

Figure 7.3 PV curve of the WSCC 9-bus load 3 using Matpower

VSAT is voltage security assessment tool developed by Powertech Labs, which runs power

flows increasing the load by the amount that the user specifies until the power flow does not converge, and during the last solutions executes modal analysis identifying which mode is affecting more the voltage instability. The results using VSAT for the WSCC 9-bus test system are shown in Table 7.3, and the PV curve of a critical load, load 3, is shown in Fig. 7.4. For running those simulation was considered that all the loads increase at the same time and in the same proportion. The initial step used to increase the load is 100 MW, and the final increment step is 10 MW. Using this software, the maximum load of the WSCC 9-bus system without contingency is 6.65 p.u, see Fig. 7.5, and the voltage collapse margin is 47%. These results differ 3% from the continuation power flow results. The reason is that the Jacobian became singular at 6.65 p.u., but the system is not unstable at that point, for that reason the modal analysis of VSAT shows a positive value at 6.65 p.u. of load, see Table 7.3.

In this way, we can state that the best solution is given by MATPOWER because it is running a continuation power flow, which indicate the maximum load that the power system can support before the voltage instability. Otherwise, with VSAT we have reasonable results, but we can not guarantee that the not convergence of the power flow gives the maximum load that the system can supply. In Table 7.3, we can see that VSAT modal analysis give a positive result in the last point of analysis [1], which means that at the maximum load the system is stable, and the maximum load can be bigger.

Table 7.3 Maximum load of the WSCC 9-bus system using VSAT

$V_{\ell 1}$	$V_{\ell 2}$	$V_{\ell 3}$	$P_{\ell max}$	$Index$	$ModalAnalysis$
0.639	0.749	0.809	6.65	47%	0.842

Values in p.u .

[1] In VSAT positive modal analysis result means stable condition, and negative means unstable conditions

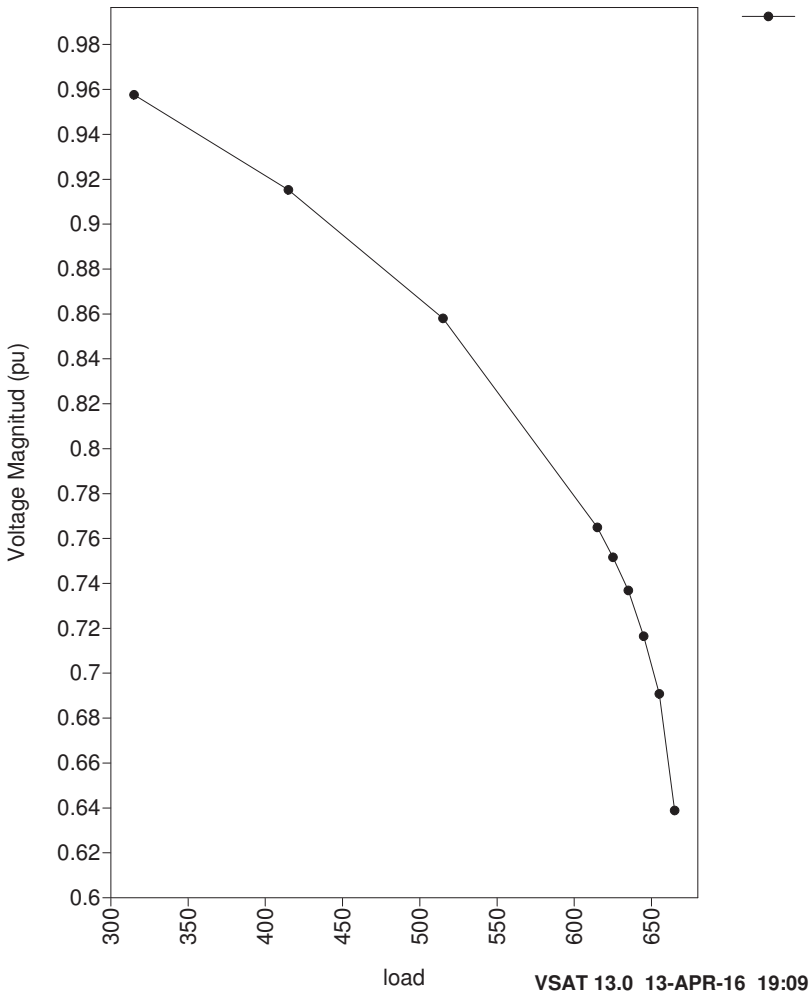

Figure 7.4 PV curve of the WSCC 9-bus load 3 using VSAT

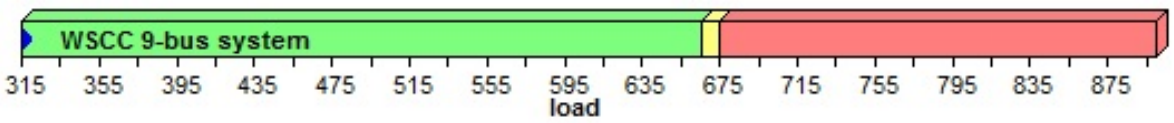

Figure 7.5 VSAT maximum load results for the WSCC 9-bus

Now, that the reduction was done for the WSCC 9 bus system without contingency, we simulate all the n-1 contingencies without shedding load to show the effect of contingencies

on the voltage stability margin, see Table 7.4. In real time, when the contingency occurs, the PMU measurements will track the changes in the complex voltage and current, then we use the methodology for reducing the corridor to a single line system and evaluate the voltage stability margin. This procedure is updating constantly to track the voltage stability margin across the transmission corridor.

The results shown in Table 7.4 show which outages can generate voltage stability problems. A 100% voltage collapse margin correspond to voltage collapse. For this system, from simulation, we consider a 60% index as a critical margin. We found that under n-1 the dangerous outages are lines 1, 3, 4, and 5. For this example, was not possible to evaluate n-2 because the voltage collapse margin is reached. In addition, it is important to clarify that this system base case is not n-1 secure, it is the reason that with only one contingency the voltage collapse margin is dangerously small.

Additionally, in Table 7.4, we evaluate the accuracy of the new methodology. We contrast the voltage stability index using the synchrophasor measurements with the answers for the stability margin obtained using the well known continuation power flow (MATPOWER). These results shown that our method for evaluating voltage stability under contingencies is a reasonable approximation, with a difference lower than 5%.

During real operation, it is desirable to take remedial action promptly tracking the voltage stability margin, covering multiple contingencies in real time. For this, is necessary to define a security limit margin, which the operator should maintain in order to avoid voltage stability problems and blackout. In the case that the limit is violated, the operator should decrease the transfer of power across the corridor or in more severe cases shed load. For example, if we consider the security margin as sixty percent, under contingency of L1, L3, L4 and L5, see Fig. 7.6, the system operator should take action in order to maintain the security level required, see Table 7.4.

For future work, we will analyze possible remedial action schemes that decrease the transfer of power across the transmission corridor in the case that the voltage stability margin will be superior to the maximum level admitted. For taking this action, the system should be self-governed for changing the dispatch of generation or in more extreme case for shedding load.

In this way, the system will overcome the outages, and voltage stability problems without blackouts. Its is important to clarify, that for implementing this type of schemes should be analyzed each specific case because it can be multiple solution for decrease the margin but it should be the more effective and economic solution.

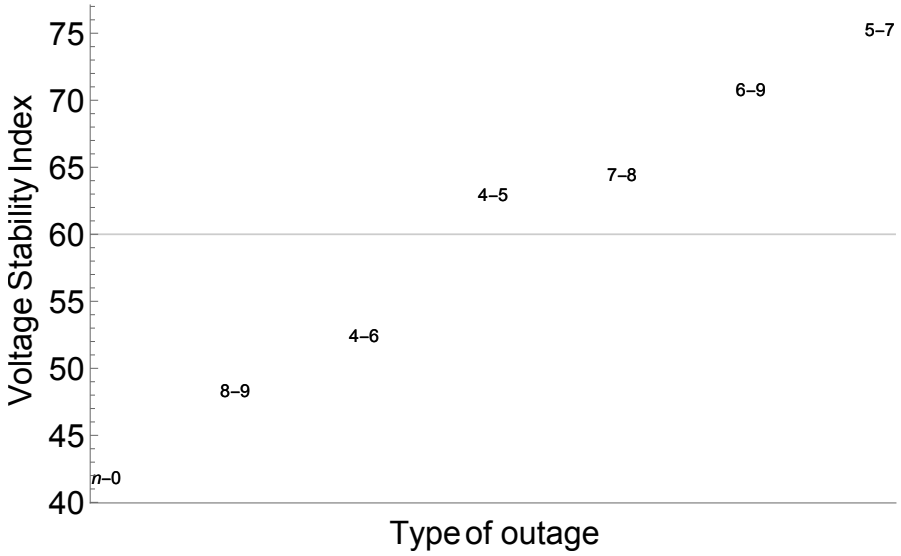

Figure 7.6 Voltage stability index under contingency of the WSCC 9-bus test system

Table 7.4 Voltage collapse margin under contingencies for WSCC 9-bus system

Line outages	Voltage stability margin (%)	
	PMUs	MATPOWER
Base case	42	44
4-5	64	70
4-6	52	57
5-7	75	70
7-8	63	57
6-9	71	67
8-9	48	50

7.3.2 Evaluation of voltage collapse margin under multiple contingencies for IEEE 25-bus test system

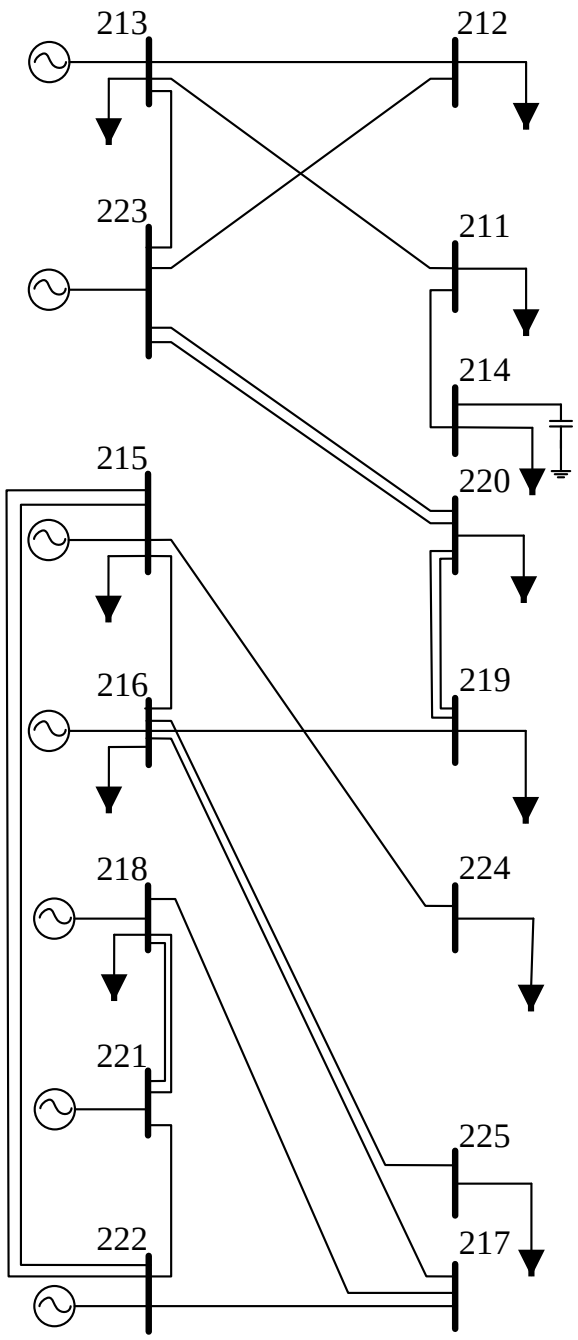

Figure 7.7 IEEE 25-bus test system corridors with seven inputs and eight outputs

We study the 230 KV grid of the IEEE 25-bus test system shown in Fig. 7.7. We divide this system into two areas, the generation area and the load area. The generation area is composed of seven buses, and the load area of eight buses. The transmission corridor is composed by twenty one lines. This system requires fifteen PMUs to measure the complex voltage and current in each bus.

First, we evaluate the voltage stability margin of the system without contingency, then we start to evaluate the voltage stability margin collapse of the system under n-1, n-2 to n-7, without shedding load or generation to show the effect of contingencies on the voltage stability margin. In Fig. 7.8, we can see how the system is going to the limit under multiple contingencies. With no contingencies the voltage stability margin is 35%, but under n-1 the index is going until 64%, n-2 to 73%, n-3 to 75%, n-5 to 87%, n-6 and n-7 to 86%. According to these results, this voltage collapse margin can be a indicator of the severity of the contingency without running any simulation, with the advantage of monitoring in real time if sudden contingencies create problems to the grid.

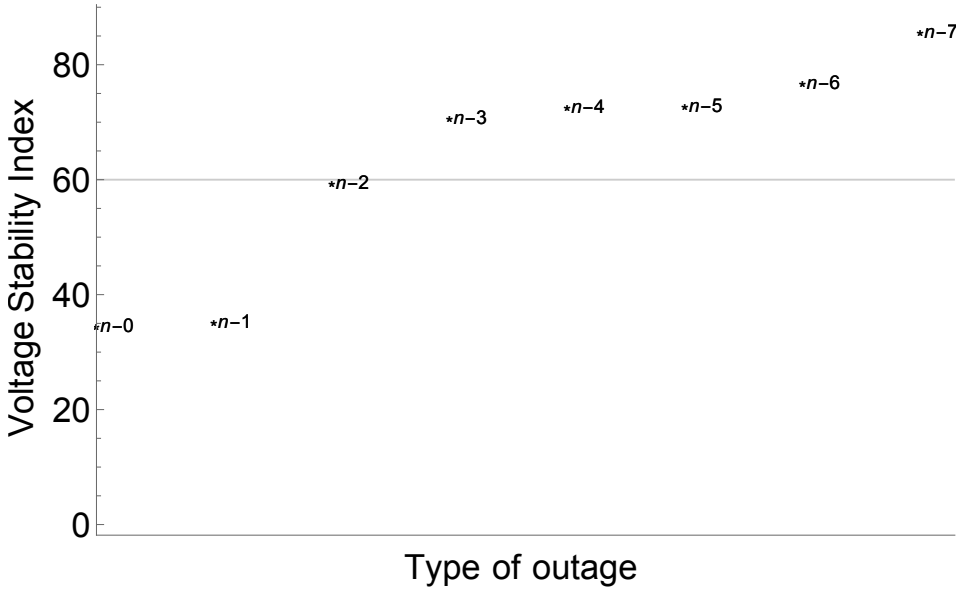

Figure 7.8 Voltage stability index under contingency of the IEEE 25-bus test system

After we monitor the voltage collapse margin without contingency, we analyze the longer cascade before reach the voltage stability margin. As we can expect, as the number of outages

increase, the system is more weak, and the voltage collapse margin is tracking this effect in the system, see Fig 7.9. This results clearly show after which outages the system can present voltage stability problems. For example, after n-2 the system exceeds the normal voltage stability margin, which means that the system has a high probability of a voltage collapse, and it require some actions to ensure an operation secure point. Those actions can be to move generation or decrease the load. For this specific case, the action should be to decrease the load.

For analyzing the voltage stability margin in which the system is stable, we analyze all the possible contingencies combinations until the system is reaching the 100% margin. From Fig 7.8, we can see all the possible cascade until reaching the 100% voltage stability margin of the IEEE 25-bus test system. For this figure, we can conclude that the n-1 contingencies are not over passing the voltage stability margin limit 60%, it is due that the system is able to continue in stable condition under n-1. However, under n-3 contingencies the voltage stability margin limit is over-passed the 60 % of the time, and for outages bigger than n-3, the limit is reached almost all the time. Whit this results, we can show the importance of tracking voltage stability online under contingencies because with many n-2 outages the system is in a critical condition which can be worst with a single outage more. Also, according to those results we can set the voltage stability alarm according to the n-1 secure results. For example in this cases 60% is a reasonable alarm, where a superior margin should be considered as an alert for taking action and prevent further problems.

7.3.3 Evaluation of voltage collapse margin under multiple contingencies for a real event of the Colombian ISO system

We study a real event of the Colombian ISO system. The event occurred in the 230 kV system of the east area. The affected area involves three generators, five loads, and a transmission corridor of fifteen lines, see Fig. 7.10. The voltage collapse margin evaluation of this system requires eight PMUs to measure the complex voltage and current in all buses bounding the transmission corridor. The event occurred on March 9 of 2011 at 17:13 hours during a thunder storm. At that time, the total demand of the Colombian system was 7395 MW, and

the demand of the area analyzed is 1200 MW of active power and 360 Mvar of reactive power, which is consumed by Bogotá, the capital city of Colombia, and near by areas.

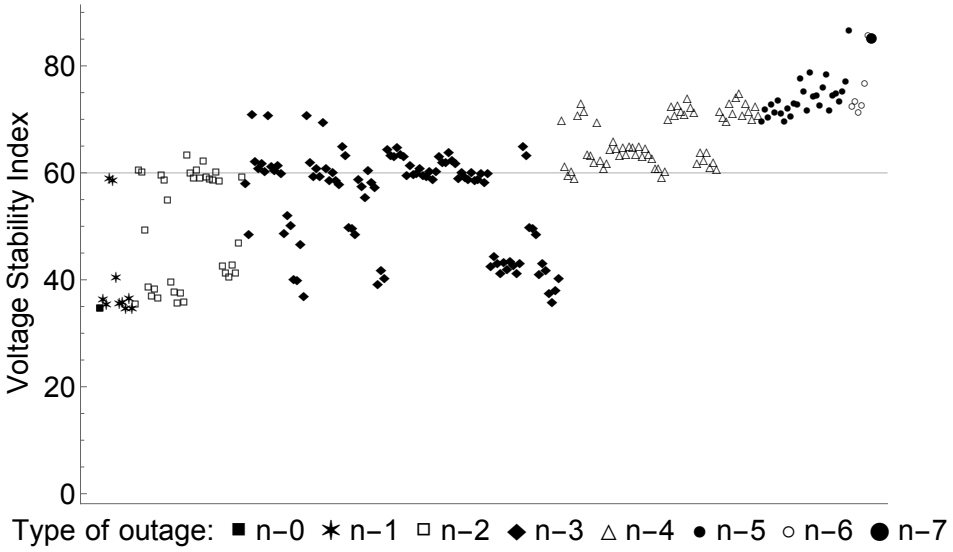

Figure 7.9 Voltage collapse margin under a multiple outages in the IEEE 25-bus

The cascade start with a lighting fault over the phase C of the line (1). Previous to the fault (1), in substation $g2$ there was a intermittent voltage signal. That intermittent signal, activated the lock function of the line (1), disabling the distance protection. When the fault on line (1) occurred, with the distance protection unavailable, all the elements connected to the substation $g2$ started to trip in order to clear the fault.

First, we evaluate the voltage stability margin of the system without a contingency, then we evaluate the voltage stability margin collapse of the system under n-1 to n-6 to show the effect of the contingencies on the voltage stability margin. In Fig. 7.11, we can see how the system is moving towards the limit under multiple contingencies. The contingencies are enumerated in Fig. 7.11, according to which line trips first. In other words, the event starts with the fault in line (1), then line (2) is disconnected, line (3), and so on. According to this order, n-2 correspond to the outage of lines (1) and (2), n-3 correspond to line outages (1), (2), (3), etc. For each n-i, where i={0,1,2,3,4,6}, we use the complex power reduction and estimate the voltage collapse margin with the power index.

As we can see in Fig. 7.11, under no contingencies the voltage stability margin was 31%,

and under n-5 the index is more than 50%, after the n-6 all the lines associated to bus $g2$ trip, shedding 440 MW in bus $g2$, 560 MW in bus $g3$ and 180 MW in the south area. With such loss of generation the frequency decrease until 59.14 Hertz, initiating the under-frequency load shedding of 660 MW. At that point the demand start to increase 100 MW, which depressed further the voltages of the area generating the trip of the plant in the bus $g1$ decreasing the frequency to 58.9 Hertz, which activated the under-frequency protections, shedding 450 MW of load, see Fig. 7.12.

For showing that the results with the online voltage stability margin can be used in the industry, we compare the results using VSAT, which is the voltage stability software used for the Colombian ISO, see Table 7.5. The index using VSAT is bigger according to the results and explanation shown in section 7.3.1. However, it is clear that the online voltage stability margin is tracking the voltage stability problems, and it can be used for prevent problems in the network.

The case analyzed is median - high demand in an area where the reliability of the system is extremely important since a large part of the Colombian economy is centralized in this area. With the voltage stability evaluation it is possible to determine if the area is in danger of a long term voltage stability problems, giving time to the operators to take action before the voltage collapse. From 7.11, we can see how the voltage stability margin is showing the potential problems, and when the operator start to see that alarm, the transfer of power should be decreased in order to restore the margin and avoid severe problems.

Those events occur in a short time, less than five minutes, thus is not possible to run simulation for taking actions, and this is where synchrophasor measurement applications can help to avoid the collapse. For example if after contingency five, the transfer power had been reduced by 300 MW, the index decrease to 10% avoiding the voltage collapse. For efficiency this voltage stability margin should be connected to a remedial action scheme that can protect the system autonomously.

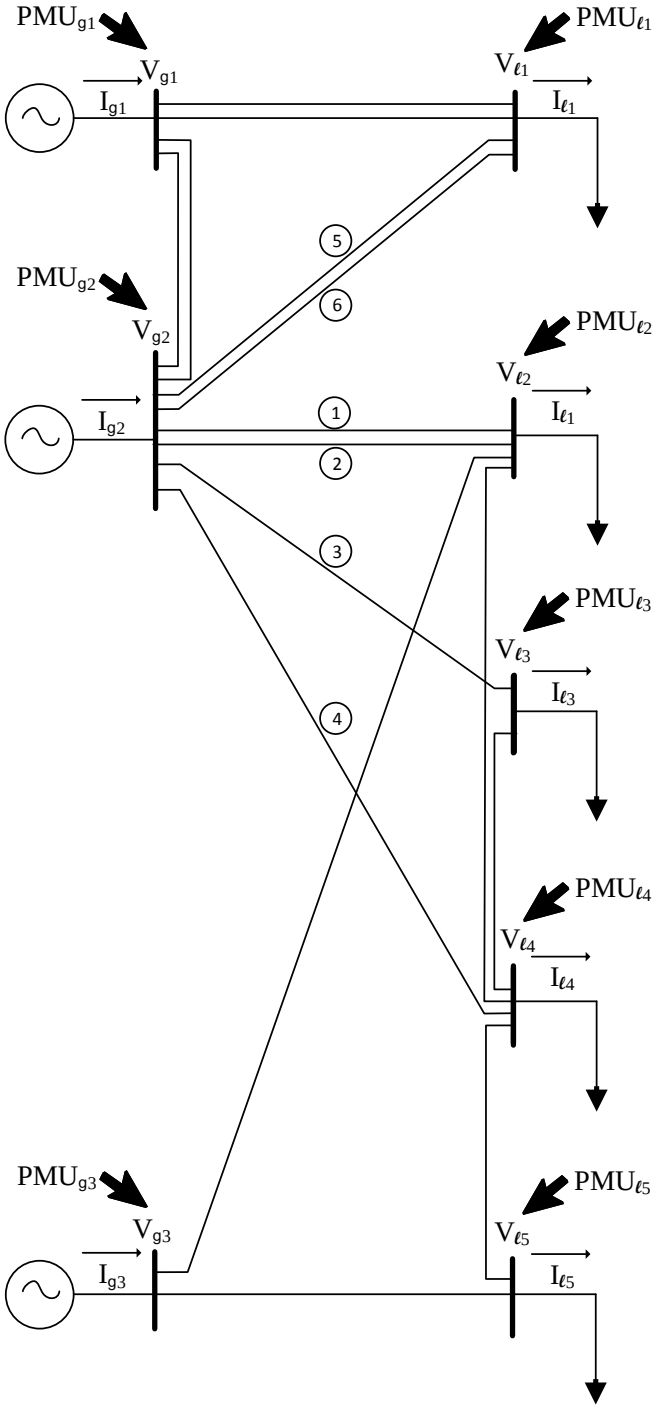

Figure 7.10 Area of the East part of the Colombian ISO system

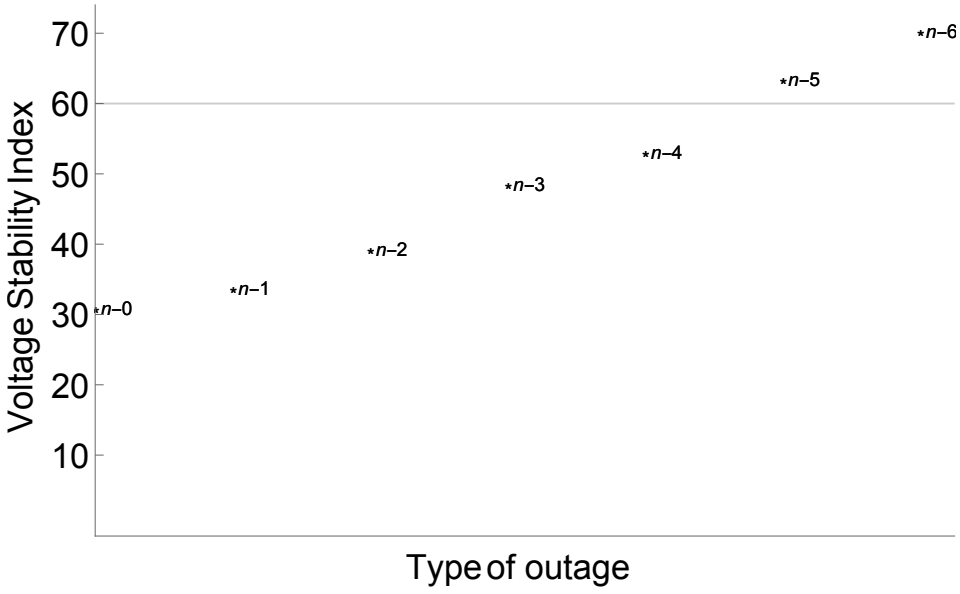

Figure 7.11 Voltage collapse margin under multiple contingencies of a real event in the Colombian ISO System

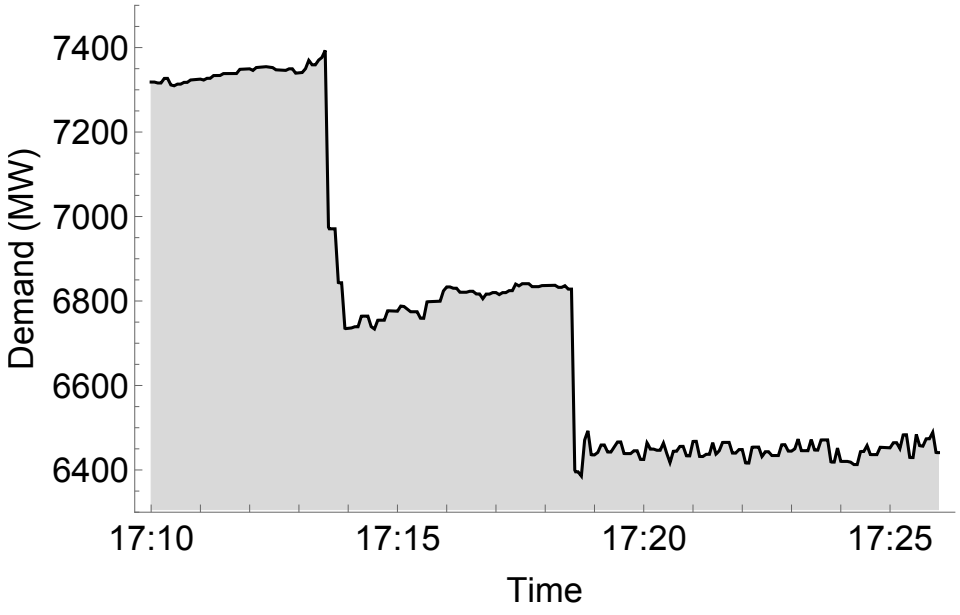

Figure 7.12 Demand curve under multiple contingencies of a real event in the Colombian ISO System

Table 7.5 Voltage collapse margin under contingencies for a real event of the Colombian ISO system

Contingency	Voltage stability margin (%)	
	PMUs	VSAT
n-0	31	39
n-1	34	41
n-2	39	50
n-3	49	59
n-4	53	60
n-5	62	73
n-6	70	79

7.4 Conclusion

We show how to reduce multiple lines in several transmission corridors to a single line equivalent to which online monitoring of voltage stability with synchrophasors can be applied. The reduction is based on synchrophasor measurements of complex power and current at both ends of the lines, and the reduction shows how to combine the synchrophasor measurements so that they are effective in monitoring voltage stability. The approach can give a fast, online indication of voltage stability that can accommodate both multiple contingencies and generator reactive power limits. These capabilities should increase operator situation awareness under emergency conditions, and should be complementary to methods that make pre-contingency calculations from a model based on the state estimator.

The complex power methodology for analyzing online voltage stability margin for multiple transmission lines and multiple contingencies was tested in the WSCC 9-bus system, IEEE 25 bus test system and in a real event of the Colombian ISO system. In addition, it is compared with commercial software VSAT, and MATPOWER, giving excellent results. Our results sug-

gest that we have found a promising and systematic approach for online monitoring of voltage stability margin for multiple transmission lines and multiple contingencies. Also the results shown that during events there is not time for running simulations and additional tools for the online monitoring voltage collapse margin are required for avoiding cascades and blackouts.

CHAPTER 8. CONTRIBUTIONS AND FUTURE RESEARCH

8.1 Contributions of this thesis

The main contribution of this thesis is an online application for fast monitoring of voltage stability for transmission corridors with multiple lines, large transfers of power, and under multiple contingencies. The benefit is the quick detection of voltage stability problems in real time, without depending on the data topology, simulations, or the state estimator, which will help the operator to respond promptly to voltage stability problems.

We propose two new methods for combining corridors with multiple transmission lines to a single line for online voltage stability monitoring using synchrophasor measurements. In addition, we propose a new voltage stability index which gives a more accurate voltage stability margin compared with current indices. We tested the two new reduction methodologies for voltage stability online monitoring and the new voltage index in several cases, including a four base system, WECC 9 bus test system, IEEE 24 bus test system, IEEE 39 bus test system, and in a real event of the Colombian system, obtaining excellent results.

For combining transmission corridors with multiple lines to a single line, we used two reductions. The first reduction is based in voltage across an area, and the second reduction is based on the preservation of complex power. We compare the voltage across an area reduction and the complex power reduction with the REI equivalent, showing that each reduction preserves different qualities so that accordingly they can have different applications. Particularly, for real time voltage stability monitoring the best reduction is the complex power reduction. For the WESCC 9 bus test system, we compare the results using the complex power PMUs methodology, VSAT and MATPOWER, getting similar results. For those reasons, we conclude that this thesis presents a new methodology for evaluating voltage stability using synchrophasor

measurements which, according to our knowledge, is the best performer, and can be applied in practical cases with useful results.

8.1.1 Detailed Contributions: Developing new methods

We develop the following:

- New method for reducing a transmission corridor to a single line.

  We discovered a new method for reducing corridors with multiple lines to a single line. This method preserves the power and current of the corridor, giving excellent results for online voltage stability monitoring. (It turns out that it has also been discovered in other contexts, (9)). This new method, according to our knowledge, is the best one for online voltage stability monitoring for complex corridors, see Chapter 3, Chapter 6.

- New voltage stability index based in the maximum power.

  In Chapter 5, we present a new voltage stability index based on the maximum power that the corridor can transfer. The new index, consider the same assumptions that the VSLBI index. However, it has better performance for tracking the voltage stability margin. Using the new index and the complex power reduction for the 4 bus test system, the voltage stability margin reduces its error from 60% to 0.8%.

- Methodology for monitoring voltage stability margin online.

  In Chapter 6, we develop a new methodology for using the reductions proposed in Chapter 3 and synchrophasor measurements, where we find the voltage stability margin for a transmission corridor with multiple lines. This procedure can be useful for control center, giving the operators awareness about the maximum power that the transmission corridor can transfer without voltage stability issues.

To realize this new work, other innovations were made:

- Including reactive limits in the model.

As generator reactive limits have a big influence in the voltage stability margin, we proposed in Chapter 6 a method for incorporating the generator reactive limits. The generator that its reaching the reactive limits is considered as a negative load in the model for evaluating voltage stability using synchrophasor measurements.

- Application of the voltage stability monitoring to corridors that include load.

  We developed a methodology for assessing voltage stability in the corridor with multiple lines, where that corridor should be composed only of transmission lines. As the power system is complex, sometimes corridors can have load that has not PMUs. Hence, we present in Chapter 3 a correction of the corridor admittance to extend the methodology for corridors that include load inside.

- Applying voltage stability margin using PMUS for multiple contingencies

  The power system must work perfectly under n-1 contingencies. However, in some cases when bad weather is present, cyber attacks, or there is a highly stressed or cascading condition, the system can have more than one forced outage. For cases that have more than one forced outage, the methodology for monitoring voltage stability margin online can help the operator track the voltage stability margin and take remedial action when necessary without further analysis.

- Voltage across area method for online voltage stability monitoring.

  Chapter 6 presents a method for online voltage stability monitoring based in the voltage across area concept. This method work very well in cases where the generation area has equal voltages and the load area has equal voltages. However, when the voltages in each area are different, this method present can have an error. In this way, we recommend for online voltage stability monitoring to use the complex power methodology, which gives better results and a smaller error.

- Comparison of the two methods for reducing corridors with multiple lines to a single line with the REI reduction.

Chapter 4 presents the REI equivalent as explained by Professor Costas Vournas from National Technical University of Athens, and documents the comparisons done in collaboration with him with the voltage across an area and complex power reductions. All the reductions preserve the currents of the complete system, but preserve different additional qualities according to the desired application. For example, for voltage collapse monitoring it is better to conserve the complex power as well the complex current.

8.1.2 Testing new methods

We tested the develop new methods in the following systems:

- Four bus system.

  We tested the following new methods:

  - The two methods for reducing corridor with multiple lines to a single line.
  - The comparison between the two reductions proposed in this thesis and the REI equivalent.
  - The comparison of the VSLBI index and the new index.
  - The generator reactive limits.

- WSCC 9 bus system

  We tested the following new methods:

  - The complex power reduction.
  - The new voltage stability index for different values of load according a load duration curve.
  - The multiple contingencies methodology.
  - The comparisons between the complex power PMU method, VSAT, and MATPOWER.

- IEEE 25 bus system.

  We tested the following new methods:

  - The complex power reduction.
  - The secure voltage stability margin according to all the possible cascades before the voltage collapse.
  - The multiple contingencies methodology.

- IEEE 39 bus system.

  We tested the following new methods:

  - The complex power reduction.
  - The new voltage stability index for different values of load according a load duration curve.

- Colombian System.

  We tested the following new methods:

  - The complex power reduction.
  - The multiple contingencies methodology.
  - The comparison between the complex power PMU method, and VSAT.

8.1.3 Papers

The following papers were published:

- C. Vournas, L. Ramirez, I. Dobson, On two bus equivalents of transmission corridors, IEEE Transaction on Power System, 2015, vol 31, pp. 2497 -2498.
- L. Ramirez, I. Dobson, Monitoring voltage collapse margin with synchrophasors across transmission corridors with multiple lines and multiple contingencies, IEEE Power Engineering Society General Meeting, Denver USA, July 2015.
- L. Ramirez, I. Dobson, Monitoring voltage collapse margin by measuring the area voltage across several transmission lines with synchrophasors, IEEE Power Engineering Society General Meeting, National Harbor MD USA, July 2014.

8.1.4 Presentations to industry

The following talks were presented to the industry:

- L. Ramirez, I. Dobson, Fast monitoring of voltage collapse margin with synchrophasors across transmission corridors with multiple lines in Colombia, International Synchrophasor Symposium, Atlanta USA, March 2016.
- L. Ramirez, Cascading outage prevention in Colombia, International Synchrophasor Symposium, Atlanta USA, March 2016.
- L. Ramirez, I. Dobson, Measuring stress across an area of a power system with area angles, Fiftieth annual report of the Electric Power Research Center, Ames IA USA, June 2013.
- L. Ramirez, I. Dobson, Monitoring voltage collapse margin by measuring the area voltage across several transmission lines with synchrophasors, Fifty-first annual report of the Electric Power Research Center, Ames IA USA, June 2014.

8.2 Future research

The thesis establishes a superior method to monitor voltage stability quickly with synchrophasor and confirms it on power systems models. Therefore, the future work would transfer the new method to the industry. In particularly, we would like to work in the following topics:

- Test the system in other real transmission corridors.

  We applied the new methodology for online voltage stability monitoring using PMUs in one sub area of the Colombian System. However, for future work we are interested in applying this new concept in other real system.

- Test the system with real PMU data.

  Until now, the methodology for monitoring voltage stability margin online has been tested in model systems and in a real corridor of the Colombian system. However, the data for

the real system was from a model of the Colombian grid. Thus for future work, we want to test this methodology with real PMU data.

- Consider implementation issues.

  This thesis does not address the implementation issues of PMUs, for many researchers are focused on those issues. However, it is important to account for errors and delays related to the measurements, communications and devices. Implementation issues may arise if the corridor is defined without perfectly following the assumptions presented in this work. For example, a corridor may have load near to the sending bus in which the constant magnitude voltages assumption is not accurate.

BIBLIOGRAPHY

[1] Ajjarapu V., and Christy C. (1992). The Continuation Power Flow: A Tool for Steady State Voltage Stability Analysis. *IEEE Trans. on Power Systems*, *7*(1).

[2] Ajjarapu V. (2007). Computational Techniques for Voltage Stability Assessment and Control. *Springer Science & Business Media*.

[3] Almeida A.B., Reginatto R., Jovita R., and Silva G.C. (2010). A software tool for the determination of dynamic equivalents of power systems. *IREP Symposium*.

[4] Alzahawi T., Sachdev M., and Ramakrishna G. (2005). A special protection scheme for voltage stability prevention. *IEEE Canadian Conference on Electrical and Computer Engineering*.

[5] Bai C., Begovic M., Nuqui R., Sobajic D., Song Y. (2013). On voltage stability monitoring with voltage instability predictors. *IREP Symposium, Bulk Power System Dynamics and Control-IX*.

[6] Balanathan R., Pahalawaththa N. C., Annakkage U. D., and Sharp P. W. (1998). Undervoltage load shedding to avoid voltage instability. *IEEE Proc. Generation, Transmission, and Distribution*, *145*(2), 175–181.

[7] Bertsch, J. (2003). Experiences with and perspectives of the system for wide area monitoring of power systems. *Quality and Security of Electric Power Delivery Systems, CIGRE/PES*.

[8] Canizares C.A., and Alvarado, F.L. (1993). Point of collapse and continuation methods for large AC/DC systems. *IEEE Trans. Power Systems*, *8*(1), 1–8.

[9] Chakrabortty A. (2011). A Measurement-Based Framework for Dynamic Equivalencing of Large Power Systems Using Wide-Area Phasor Measurements. *IET Generation, Transmission & Distribution*, *2*(1), 68–81.

[10] Chiang, H.-D., Dobson, I., Thomas, R.J., Thorp, J.S., and Fekih-Ahmed, L. (1990). On voltage collapse in electric power systems. *IEEE Trans. Power Systems*, *5*(2), 601–611.

[11] Corsi S. (2010). Wide area voltage protection. *IEEE Trans. Smart Grid*, *4*(10), 1164–1179.

[12] Darvishi, A. (2016). Threshold-Based Monitoring of Multiple Outages With PMU Measurements of Area Angle. *IEEE Trans. Power Systems*, *31*(3), 2116–2124.

[13] Dimo, P. (1975). Nodal Analysis of Power Systems. *Abacus Press.*

[14] Dobson I. (1992). Observations on the geometry of saddle node bifurcation and voltage collapse in electrical power systems. *IEEE Transactions on Circuits and Systems I: Fundamental Theory and Applications*, *39*(3), 1057–7122.

[15] Dobson I. (1994). The Irrelevance of Load Dynamics for the Loading Margin to Voltage Collapse and Its Sensitivities. *Bulk Power System Voltage Phenomena-III, Voltage Stability, Security and Control.*

[16] Dobson I. (2011). The irrelevance of electric power system dynamics for the loading margin to voltage collapse and its sensitivities. *Nonlinear Theory and Its Applications, IEICE*, *2*(3), 263–280.

[17] Dobson I. (2012). Voltages across an area of a network. *IEEE Trans. Power Systems*, *27*(1), 993–1002.

[18] Duong D., and Uhlen K. (2008). Phasor measurement application for power system voltage stability monitoring. *Power and Energy Society General Meeting.*

[19] Duong D., and Uhlen K.(2013). Online voltage stability monitoring based on PMU measurements and system topology. *Third International Conference Electric Power and Energy Conversion Systems.*

[20] Ejebe, G.C. and Van Meeteren, H.P. and Wollenberg, B.F.(1988). Fast contingency screening and evaluation for voltage security analysis. *IEEE Trans. Power Systems.*

[21] Flueck, A.J. and Gonella, R. and Dondeti, J.R. (2002). A new power sensitivity method of ranking branch outage contingencies for voltage collapse. *IEEE Trans. Power Systems.*

[22] Genet B., Sezi T., and Maun J-C. (2008). Comparison of Thévenin's equivalent based methods to monitor voltage stability. *16th Power System Computation Conference (PSCC).*

[23] Glavic M., and Van Cutsem T. (2008). Detecting with PMUs the onset of voltage instability caused by a large disturbance. *IEEE PES General Meeting.*

[24] Glavic M., and Van Cutsem T. (2011). A short survey of methods for voltage instability detection. *IEEE PES General Meeting.*

[25] Glavic M., Quanta Technol LLC, Raleigh NC USA, Lelic M., Novosel D., Heredia E.,and Kosterev D.N. (2012). A simple computation and visualization of voltage stability power margins in real-time. *IEEE PES Transmission and Distribution Conference and Exposition (T&D).*

[26] Golubitsky M., and Schaeffer D. (1984). Singularities and Groups in Bifurcation Theory. *Springer-Verlag.*

[27] Greene S. (1993). Constraint at a saddle node bifurcation. *MS thesis, Univ. of Wisconsin-Madison.*

[28] Greene S., Dobson I., and Alvarado F. (1997). Sensitivity of loading margin to voltage collapse with respect to arbitrary parameters. *IEEE Trans. Power Systems*, *12*(1), 262–272.

[29] Greene, S. and Dobson, I. and Alvarado, F.L. (1999). Contingency ranking for voltage collapse via sensitivities from a single nose curve. *IEEE Trans. Power Systems*, *14*(1), 232-240.

[30] Hadjsaid, N. and Benahmed, M. and Fandino, J. and Sabonnadiere, J.C. and Nerin, G. (1993). Fast contingency screening for voltage-reactive considerations in security analysis. *IEEE Trans. Power Systems*, *8*(1), 144-151.

[31] Hauer, J., Mittelstadt, W., Martin, K., Burns, J., Lee, H., Pierre, J., and Trudnowski, D. (2009). Use of the WECC WAMS in wide-area probing tests for validation of system performance and modeling. *IEEE Trans. Power Systems*, *24*(1), 250-257.

[32] Heng-Yi S., Yi-Ting C., and Chih-Wen L. (2012). Estimation of Voltage Stability Margin Using Synchrophasors. *IEEE PES General Meeting*.

[33] IEEE Power Engineering Society, Power System Stability Subcommittee, IEEE Power Engineering Society. (2002). Voltage Stability Assessment: Concepts, Practices and Tools. *IEEE-PES*.

[34] Jang W., Mohapatra S., Overbye, T. J., and Zhu H. (2013). Line limit preserving power system equivalent. *Proc. IEEE Power Energy Conf.*.

[35] Larsson M., Rehtanz C., and Bertsch J. (2003). Monitoring and operation of transmission corridors. *IEEE PowerTech Conference*.

[36] Massucco S., Grillo S., Pitto A., and Silvestro F. (2009). Evaluation of Some Indices for Voltage Stability Assessment . *IEEE Power Tech Conference*.

[37] McCalley, J. D., Dorsey, J. F., Luini, J. F., Mackin, R. P., and Molina, G. H. (1993). Subtransmission reduction for voltage instability analysis. *IEEE transactions on power systems*. *8*(1), 349-356.,

[38] Milosevic B., and Begovic M. (2003). Voltage-stability protection and control using a wide-area network of phasor measurements. *IEEE Trans. Power Systems*, *18*(1), 121–127.

[39] Mingsong Liu L., Boming Z., Liangzhong Y., Min H., Hongbin S.,and Wenchuan W. (2008). PMU Based Voltage Stability Analysis for Transmission Corridors. *Electric Utility Deregulation and Restructuring and Power Technologies,Third International Conference*.

[40] Nara, K., Tanaka, K., Kodama, H., Shoults, R.R., Chen, M.-S., Van Olinda, P., and Bertagnolli, David. (1985). On-Line Contingency Selection Algorithm for Voltage Security Analysis. *IEEE Power Engineering Review.*

[41] Novosel D., Vu K. T., Hart D.,and Udren E. (1996). Practical protection and control strategies during large power-system disturbances. *IEEE Transmission and Distribution Conference.*

[42] Novosel D., Vu K., Centeno V., Skok S., and Begovic M. (2007). Benefits of Synchronized-Measurement Technology for Power-Grid Applications. *40th Annual Hawaii International Conference on System Sciences.*

[43] Novosel D., Quanta Technol., Bhargava B., Khoi V., and Cole J. (2008). Dawn of the grid synchronization. *IEEE Power and Energy Magazine*, *6*(1), 49–60.

[44] Podmore, R., and Germond, A. (1977). Development of dynamic equivalents for transient stability studies. *Final report (No. EPRI-EL-456). Systems Control, Inc., Palo Alto, CA (USA).*

[45] Ramirez L., and Dobson I., (2014). Monitoring voltage collapse margin by measuring the area voltage across several transmission lines with synchrophasors. *Power and Energy Society General Meeting.*

[46] Ramirez L., and Dobson I., (2015). Monitoring voltage collapse margin with synchrophasors across transmission corridors with multiple lines and multiple contingencies. *Power and Energy Society General Meeting.*

[47] Smon I., Verbic G., and Gubina F. (2006). Local voltage-stability index using Tellegen's theorem. *IEEE Trans. Power Systems*, *21*(3), 1267–1275.

[48] Sobhy M., Abdelkader, John Morrow D. (2012). Online Tracking of Thévenin Equivalent Parameters Using PMU Measurements. *IEEE Trans. on Power Systems*, *27*(2), 29–37.

[49] Van Cutsem T., and Vournas C. (1998). Voltage Stability of Electric Power Systems. *Springer Science & Business Media.*

[50] Van Cutsem T., and Vournas C. (2013). Voltage Stability of Electric Power Systems. *International Conference on Power, Energy and Control.*

[51] Venkatasubramanian V., Xing L., Guoping L., Qiang Z., and Michael S. (2011). Overview of Wide-Area Stability Monitoring Algorithms in Power Systems using Synchrophasors. *American Control Conference (ACC).*

[52] Vournas, C.D. and Ramirez, L. and Dobson, I. (2015). On Two-Bus Equivalents of Transmission Corridors. *IEEE Transactions on Power Systems.*

[53] Vu K., Begovic M., Novosel D., and Saha M. (1999). Use of local measurements to estimate voltage-stability margin. *Power Industry Computer Applications Conference (PICA).*

[54] Ward, J.B.(1949). Equivalent circuits for power flow studies. *AIEE Trans. Power Appl. Syst..*

[55] Warland L., and Holen A. T.(2002). Estimation of distance to voltage collapse: Testing an algorithm based on local measurements. *Power Systems Computation Conference.*

[56] Wei Qiu and Flueck, A.J. (2004). A new technique for evaluating the severity of generator outage contingencies based on two-parameter continuation. *IEEE PES Power Systems Conference and Exposition.*

[57] Wu, F. F., and Monticelli, A. (1983). Critical review of external network modelling for online security analysis. *International Journal of Electrical Power and Energy Systems*, *5*(24), 222–235.

[58] Zima M., and Krause T., and Andersson G. Evaluation of system protection schemes, wide area monitoring and control systems. *Sixth International Conference on Advances in Power System Control, Operation and Management.*

[59] Zimmerman R. D., and Murillo-Sanchez C. E., and Thomas R. J. (2011). MATPOWER: Steady-State Operations, Planning and Analysis Tools for Power Systems Research and Education. *IEEE Transactions on Power Systems*.